



Uni Essen and ITP preprint
cond-mat/0110011
September 30, 2001

Interacting Crumpled Manifolds

Henryk A. Pinnow¹ and Kay Jörg Wiese^{1,2*}

¹ Fachbereich Physik, Universität Essen, 45117 Essen, Germany

² ITP, Kohn Hall, University of California at Santa Barbara, CA 93106-4030, USA

Abstract

In this article we study the effect of a δ -interaction on a polymerized membrane of arbitrary internal dimension D . Depending on the dimensionality of membrane and embedding space, different physical scenarios are observed. We emphasize on the difference of polymers from membranes. For the latter, non-trivial contributions appear at the 2-loop level. We also exploit a “massive scheme” inspired by calculations in fixed dimensions for scalar field theories. Despite the fact that these calculations are only amenable numerically, we found that in the limit of $D \rightarrow 2$ each diagram can be evaluated *analytically*. This property extends in fact to any order in perturbation theory, allowing for a summation of all orders. This is a novel and quite surprising result. Finally, an attempt to go beyond $D = 2$ is presented. Applications to the case of self-avoiding membranes are mentioned.

Keywords: polymer, polymerized membrane, renormalization group, exact resummation.

Submitted to Journal of Physics

*Email: pinnow@theo-phys.uni-essen.de, wiese@itp.ucsb.edu

Contents

1	Introduction	3
2	Model and physical observables	5
2.1	The model	5
2.2	Repulsive force exerted by a membrane on a wall	8
2.3	Unbinding transition	9
3	Operator product expansion and one-loop result	11
4	Two-loop calculation in a MS-scheme	15
4.1	Operator product expansion	15
4.2	Numerical calculation in $0 < D < 2$	16
4.3	RG-function and extrapolation	19
5	Calculation in fixed dimension: The massive scheme	22
5.1	Phantom manifolds	22
5.2	Self-avoiding membranes	22
6	Summation of the perturbation series in the limit $D = 2$	24
6.1	N -loop order	24
6.2	The limit $D \rightarrow 2$ and $(2-D)$ -expansion	25
6.3	Asymptotic behavior of the series	29
6.4	The RG-functions in the bare coupling	31
6.5	Calculation in the renormalized coupling	33
6.6	An instructive case: $d = 0$	35
7	Discussion and conclusion	35
A	Universal $1/r$ - repulsion law for polymers	36
B	Conformal mapping of the sectors	38
R	References	41

1 Introduction

Interacting lines and more generally manifolds play an important role in many areas of modern physics. Examples of lines are self-avoiding polymers [1], vortex-lines in super-conductors [2], directed polymers in a disordered environment, also equivalent to surface growth [3], diffusion of particles and many more. Generalizing results to membranes often poses severe problems, but also new insight into physics. Recently, a lot of work has been devoted to self-avoiding membranes (see [4] for a review). Applications reach as far as high-energy physics, where strings and M-branes have been proposed as a general framework for unifying all fundamental interactions.

In this article, we focus on the statistical physics of systems without disorder. We think of situations like the binding and unbinding of a long chain as e.g. a polymer or a membrane on a wall or the wetting of an interface. More precisely, we study the interaction of a single freely fluctuating manifold with another non-fluctuating, fixed object. Depending on whether the interaction is attractive or repulsive, one can distinguish two different scenarios: One may either observe a delocalization transition from an attractive substrate as in wetting phenomena or steric repulsions by a fluctuating manifold. Both cases have in common that excluded volume effects become important. The situation for polymers or a 1-dimensional interface is relatively simple: One knows that in this case polymers interacting with a defect or a wall (excluding or not half of the space) as well as short-range critical wetting are in the same universality class [5,6]. For two-dimensional interfaces, the situation is more complicated, and a lot of effort has been spent to understand e.g. the delocalization transition [7–14]. Particularly, one is interested in critical wetting for the case of a short-ranged interaction potential. Then, it can not be approximated by a polynomial in the field \vec{r} and the conventional field-theoretic approach known from ϕ^4 -theory fails. This led to a couple of different ansätze [8,9,11–13], among others the functional renormalization group approach of [12,13].

Here we follow a different route: We start by constructing a *systematic perturbative* renormalization group treatment of the delocalization transition as well as the universal repulsive force exerted by a membrane on a point, line or more generally hyper-plane like defect. We therefore introduce a flexible “phantom” manifold of internal dimension $0 \leq D \leq 2$. By introducing a δ -potential in a subspace \mathcal{E} of dimension d' , part of the embedding space $\mathbb{R}^{d+d'}$ (see fig. 1.1) we punish configurations crossing \mathcal{E} . Neglecting the effect of self-avoidance between

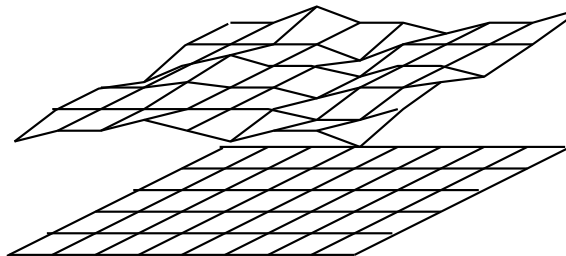


Figure 1.1: A fluctuating membrane interacting by excluded volume with a surface-like defect.

distinct points within the fluctuating manifold, the free energy of a given configuration reads:

$$\mathcal{H}[\vec{r}] = \int_{x \in \mathcal{M}} d^D x \frac{1}{2} (\nabla \vec{r}(x))^2 + g_0 \int_{x \in \mathcal{M}} d^D x \int_{\vec{y} \in \mathcal{E}} d^{d'} \vec{y} \delta^{d+d'}(\vec{r}(x) - \vec{y}), \quad (1.1)$$

where $\vec{r}(x)$ is the position of monomer $x \in \mathcal{M}$ in embedding space $\mathbb{R}^{d+d'}$, and \mathcal{M} denotes the D -dimensional coordinate space of the manifold. In the case of a polymer this is simply the internal chain length. g_0 is the attractive or repulsive interaction, of dimension (in inverse length-units)

$$\varepsilon(D, d) := [g_0] = D - \frac{2-D}{2}d. \quad (1.2)$$

The interaction is naively relevant in the infrared for ε positive, and irrelevant for ε negative. In a perturbative treatment, ε is the natural expansion parameter. The situation is similar to self-avoiding membranes and thus (1.1) has been studied as a “toy-model” for the analysis of the renormalizability of the more complicated interaction in the generalized Edwards model for self-avoiding polymerized membranes [15–17]. It was shown to be renormalizable for arbitrary manifold dimensions $0 < D < 2$ [16,17]. This means that the large scale properties are universal, i.e. do neither depend on the regularization scheme used in these calculations, nor on the form of the contact interaction, as long as it is short-ranged. Universal quantities have thus been obtained to one-loop order. They are related, as we will show below, to the correction to scaling exponent ω , which as usually in critical phenomena contains deviations from the long-distance scaling behavior. Neglecting self-interactions, one has to distinguish between polymers, which are always crumpled and membranes, for which a highly folded high-temperature state is separated through a crumpling transition from an essentially flat low-temperature phase [18–21]. The effect of self-avoidance can also be taken into account [22–25,4]. It has been shown to lead as in the case of polymers to a swelling of the membrane and correspondingly to a non-trivial exponent for the radius of gyration [26,27]. However, it is not clear whether a fractal phase can be found in experiments or simulations. (See [28] for the latest simulations). In this work we will mostly neglect self-avoidance.

The aim of this article is two-fold: First, we present the necessary techniques to treat the model (1.1) beyond the leading order. We explicitly perform a two-loop calculation which gives the correction to scaling exponent ω at order ε^2 . Specializing to membranes one finds that the 2-loop result naively diverges in the limit of $D \rightarrow 2$. This is a problem of the ε -expansion, since there, diagrams have to be evaluated at $\varepsilon(D, d_c(D)) = 0$, and taking $D \rightarrow 2$ implies $d_c(D) \rightarrow \infty$ causing the result to diverge. This motivated us to try a “massive scheme” in fixed dimension, i.e. finite ε . It turns out that the limit $D \rightarrow 2$ can then be taken and is regular. Even more, the 2-loop diagram, which for $D < 2$ can only be calculated numerically, can now be evaluated *analytically*. This striking property even holds for higher orders, and we are able to give an explicit – quite simple – expression for the perturbation series. Then the whole series can be summed and the strong coupling limit analyzed. This is one of the very few cases where one can indeed obtain the *exact* relation between bare and renormalized coupling in the limit of $D \rightarrow 2$, and thus the *exact* β -function. This result does not depend on the explicit regularization and renormalization prescriptions, and is also obtained for a membrane of spherical or toroidal topology. In a final step, we lay the foundations for an expansion about $D = 2$. In contrast to the leading order, the first order corrections already depend on the cut-off procedure. We study one specific procedure, which turns out to reproduce results for polymers at leading order

approximately, and even exactly in $d = 0$. Work is in progress to obtain a more systematic expansion about $D = 2$ [29].

2 Model and physical observables

2.1 The model

We start from the manifold Hamiltonian (1.1). We split the total embedding space $\mathbb{R}^{d+d'}$ into \mathcal{E} and its orthogonal complement \mathcal{E}_\perp of dimension d . Each $x \in \mathcal{V}$ points to a point $\vec{r}(x) = (\vec{r}_\perp(x), \vec{r}_\parallel(x))$, with $\vec{r}_\parallel(x) \in \mathcal{E}$ and $\vec{r}_\perp(x) \in \mathcal{E}_\perp$. The integration over the subspace \mathcal{E} is then trivial and gives

$$\int_{\vec{y} \in \mathcal{E}} \delta^{d+d'}(\vec{r}(x) - \vec{y}) = \delta^d(\vec{r}_\perp(x)). \quad (2.1)$$

In the partition function

$$\mathcal{Z}_{\text{total}} = \int \mathcal{D}[\vec{r}] \exp(-\mathcal{H}[\vec{r}]) \quad (2.2)$$

the contributions from the parallel and orthogonal components of $\vec{r}(x)$ factorize as

$$\mathcal{Z}_{\text{total}} = \mathcal{Z}_0 \times \mathcal{Z}(g_0) \quad (2.3)$$

with

$$\mathcal{Z}_0 = \int \mathcal{D}[\vec{r}_\parallel] \exp\left(-\frac{1}{2}(\nabla_\parallel \vec{r}(x))^2\right) \quad (2.4)$$

$$\mathcal{Z}(g_0) = \int \mathcal{D}[\vec{r}_\perp] \exp(-\mathcal{H}_\perp[\vec{r}_\perp]) \quad (2.5)$$

$$\mathcal{H}_\perp[\vec{r}_\perp] = \int_{\mathcal{M}} d^D x \left(\frac{1}{2}(\nabla \vec{r}_\perp(x))^2 + g_0 \delta^d(\vec{r}_\perp(x)) \right). \quad (2.6)$$

Since \mathcal{Z}_0 is trivial, we will only consider $\mathcal{H}_\perp[\vec{r}_\perp]$ and shall drop the subscript \perp for notational simplicity. We keep in mind that cases with $d < D$ make sense, for instance a polymerized (non-selfavoiding) membrane interacting with a wall is described by (2.6) setting $D = 2$ and $d = 1$.

Let us discuss (2.6) in more detail: The first term is the elastic energy of the manifold which is entropic in origin. We have scaled elasticity and temperature to unity. The second term models the interaction of the manifold with a single point at the origin in the external d -dimensional space, but we remind that the physical interpretation may well be that of a line or surface. The coupling constant g_0 may either be positive (repulsive interaction) or negative (attractive interaction). We now give the dimensional analysis. In coordinate-space units, the engineering dimensions are

$$\begin{aligned} \dim[x] &= 1 \\ \nu &:= \dim[\vec{r}] = \frac{2-D}{2} \\ \varepsilon &:= \dim \left[\int_{\mathcal{M}} d^D x \delta^d(\vec{r}(x)) \right] = D - \nu d \end{aligned} \quad (2.7)$$

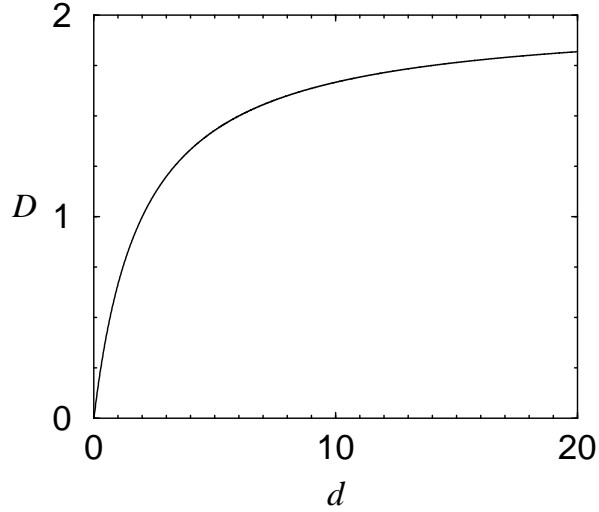


Figure 2.1: Critical line defined through $\varepsilon = 0 \Leftrightarrow d_c(D) = \frac{2D}{2-D}$. The interaction is relevant for points that lie above that line.

$$g_0 \sim \mu^\varepsilon$$

$$\dim[\mu] = -1 ,$$

where

$$\mu \equiv \frac{1}{L} \tag{2.8}$$

is an inverse length scale. The interaction is naively relevant for $\varepsilon > 0$, i.e. $d < d_c$ with (see figure 2.1)

$$d_c = \frac{2D}{2-D} , \tag{2.9}$$

irrelevant for $\varepsilon < 0$ and marginal for $\varepsilon = 0$. It has been shown [16,17] that the model is renormalizable for $0 < D < 2$ and $\varepsilon \geq 0$. Results for negative ε are obtained via analytical continuation. One can define the renormalized coupling g as

$$g := \frac{\mathcal{N}}{\mathcal{V}_{\mathcal{M}}} [\mathcal{Z}(0) - \mathcal{Z}(g_0)] L^\varepsilon , \tag{2.10}$$

where the normalization \mathcal{N} depends on the definition of the path-integral (but not on L) and is chosen such that

$$g = g_0 L^\varepsilon + O(g_0^2) . \tag{2.11}$$

Universal quantities are obtained at fixed-points of the β -function, which is defined as

$$\beta(g) := \mu \left. \frac{\partial g}{\partial \mu} \right|_{g_0} . \tag{2.12}$$

The β -function thus describes, how the effective coupling g changes under scale transformations, while keeping the bare coupling g_0 fixed. Let us already anticipate the 1-loop result,

which we derive later. It reads

$$\beta(g) = -\varepsilon g + \frac{1}{2}g^2 + O(g^3), \quad (2.13)$$

where g is the dimensionless renormalized coupling. Apart from the trivial solution, $g = 0$, the flow equation given by (2.12) and (2.13) has a non-trivial fixed point at the zero of the β -function

$$g^* = 2\varepsilon + O(\varepsilon^2). \quad (2.14)$$

We shall show below that the scaling behavior is described by the slope of the RG-function at the fixed point, which is universal as a consequence of renormalizability. The long-distance behavior is then governed by the δ -interaction as considered in our model (2.6), which is the most relevant operator at large scales. Let us now discuss possible physical situations (see fig. 2.2):

- (a) $\varepsilon > 0$: The RG-flow has an infrared stable fixed point at $g^* > 0$ and an IR-unstable fixed point at $g = 0$. The latter describes an unbinding transition whose critical properties are given by the non-interacting system, while the non-trivial IR stable fixed point determines the long-distance properties of the delocalized state, the long-range repulsive force exerted by the fluctuating manifold on the origin – which we remind may be a point, a line or a plane.
- (b) $\varepsilon < 0$: Now, the long-distance behavior is Gaussian, while the unbinding transition occurs at some finite value of the attractive potential, $g^* < 0$, which corresponds to an infrared unstable fixed point of the β -function. Below g^* the manifold stays always attracted.
- (c) $\varepsilon = 0$: This is the marginal situation, where the transition takes place at $g^* = 0$; we expect logarithmic corrections to scaling.

Note that in the presence of an impenetrable wall constraining the configurational space strictly to half of the embedding space, the above considerations should still apply, when shifting the interaction strength appropriately. We shall discuss that in 2.3.

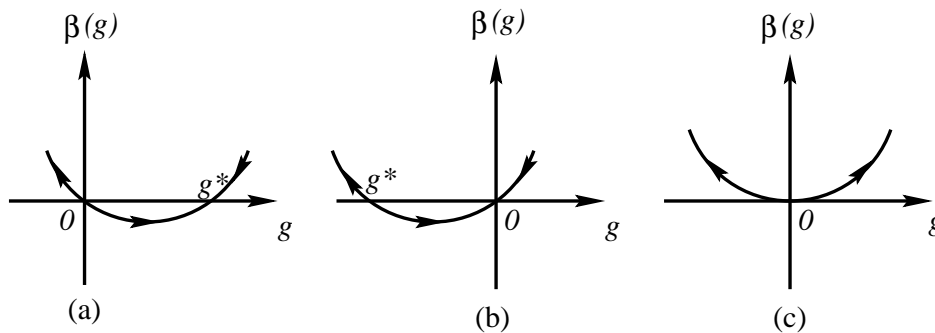


Figure 2.2: RG-function and flow for increasing manifold size L for the dimensionless renormalized coupling g : (a) in the case $\varepsilon > 0$, (b) in the case $\varepsilon < 0$, (c) in the case $\varepsilon = 0$.

2.2 Repulsive force exerted by a membrane on a wall

Since we are mainly interested in the long-distance properties of membranes for which always $\varepsilon > 0$ (this is (a) on fig. 2.2), let us try to calculate the repulsive force exerted by the membrane on the origin in the case that this point is strictly forbidden. We will derive a universal expression for this force [17]. We need the (not normalized) membrane density at position \vec{r}

$$\mathcal{Z}(\vec{r}, g_0) := \frac{1}{\mathcal{V}_{\mathcal{M}}} \int \mathcal{D}[\vec{r}] \int_{\mathcal{M}} d^D x \delta^d(\vec{r}(x) - \vec{r}) \exp[-\mathcal{H}]. \quad (2.15)$$

Since the δ -interaction also appears in \mathcal{H} , we can relate the density at the origin to the derivative of the partition function with respect to g_0 :

$$\mathcal{Z}(\vec{0}, g_0) = - \left. \frac{1}{\mathcal{V}_{\mathcal{M}}} \frac{\partial}{\partial g_0} \right|_L \mathcal{Z}(g_0) = \frac{1}{\mathcal{N}} \left. \frac{\partial(gL^{-\varepsilon})}{\partial g_0} \right|_L, \quad (2.16)$$

where g is the renormalized or effective coupling defined in (2.10). Since $\mathcal{Z}(\vec{0}, g_0)$ is dimensionless, it depends on the dimensionless combination $g_0 L^\varepsilon$ (and ε) only. Using $\mu = 1/L$, we obtain

$$\mathcal{N} \mathcal{Z}(\vec{0}, g_0) = L^{-\varepsilon} \left. \frac{\partial g}{\partial g_0} \right|_L \equiv - \frac{\beta(g)}{\varepsilon g_0 L^\varepsilon}. \quad (2.17)$$

For the further considerations, it is sufficient to know the behavior of the β -function close to the nontrivial zero. Expanding about $g=g^*$, we have

$$\beta(g) = (g - g^*)\omega(g^*) + O((g - g^*)^2). \quad (2.18)$$

Combining (2.16), (2.17) and (2.18), we get

$$\left. \frac{\partial g}{\partial(g_0 L^\varepsilon)} \right|_L = - \frac{\beta(g)}{\varepsilon g_0 L^\varepsilon} = - \frac{(g - g^*)\omega(g^*)}{\varepsilon g_0 L^\varepsilon}. \quad (2.19)$$

The solution of this differential equation is

$$g - g^* \sim (g_0 L^\varepsilon)^{-\omega(g^*)/\varepsilon} + \dots. \quad (2.20)$$

Using (2.17), this implies the scaling law

$$\mathcal{Z}(\vec{0}, g_0) \sim (g_0^{1/\varepsilon} L)^{-\omega(g^*)-\varepsilon}. \quad (2.21)$$

We now use this result to derive a scaling law for $\mathcal{Z}(\vec{r}, g_0)$, with $\vec{r} \neq \vec{0}$. In addition to $g_0 L^\varepsilon$ (and ε), $\mathcal{Z}(\vec{r}, g_0)$ depends on \vec{r} ; taking into account rotational symmetry and dimensionality, it depends on \vec{r} only through the dimensionless combination r/L^ν , with $r = |\vec{r}|$:

$$\mathcal{Z}(\vec{r}, g_0) = \mathcal{Z}(r/L^\nu, g_0 L^\varepsilon). \quad (2.22)$$

For $\mathcal{Z}(\vec{r}, g_0)$, the most interesting limit is that of $g_0 \rightarrow \infty$. Physically, this corresponds to strictly forbidding monomers to be at the origin. Therefore it is clear that this limit is well-behaved, and

$$\mathcal{Z}_\infty(r/L^\nu) := \lim_{g_0 \rightarrow \infty} \mathcal{Z}(r/L^\nu, g_0 L^\varepsilon) \quad (2.23)$$

is finite. In order to be consistent with (2.21) it has to obey a power law in the scaling regime $r \ll L^\nu$

$$\mathcal{Z}_\infty(r/L^\nu) \sim (r/L^\nu)^\theta . \quad (2.24)$$

Comparing the L -dependence of $\mathcal{Z}_\infty(r/L^\nu)$ and $\mathcal{Z}(\vec{0}, g_0)$, we obtain the exponent identity

$$\theta = \frac{\varepsilon + \omega(g^*)}{\nu} . \quad (2.25)$$

Finally, from (2.24) we derive the repulsive force between the origin and the manifold

$$\vec{f}(\vec{r}) = \nabla_{\vec{r}} \ln \mathcal{Z}_\infty(|\vec{r}|/L^\nu) = \theta \frac{\vec{r}}{r^2} . \quad (2.26)$$

Note that to derive this result, $k_B T$ has been set to 1. Reestablishing the temperature-dependence, we find

$$\vec{f}(\vec{r}) = k_B T \theta \frac{\vec{r}}{r^2} . \quad (2.27)$$

Also note that this argument gives $\theta = 0$ at the Gaussian fixed point, which is necessary since for $g_0 = 0$ no force is exerted on the membrane.

2.3 Unbinding transition

Let us discuss the physical situation at the UV-stable fixed point in figure 2.2. The fixed point corresponds to a *delocalization transition* of the manifold, which is at vanishing coupling $g^* = 0$ for $\varepsilon > 0$ and at some finite attractive coupling $g^* < 0$ for $\varepsilon < 0$.

In the localized phase $g < g^*$, correlation functions such as $\langle [\vec{r}(x) - \vec{r}(y)]^2 \rangle$ and the associated correlation length ξ_{\parallel} (in the D -dimensional internal space) should be finite, as well as the radius of gyration ξ_{\perp} . Approaching the transition point these quantities diverge as [14]

$$\xi_{\parallel} \sim (g^* - g)^{-\nu_{\parallel}} , \quad \xi_{\perp} \sim (g^* - g)^{-\nu_{\perp}} . \quad (2.28)$$

Since $\xi_{\perp} \sim \xi_{\parallel}^{\nu}$, the exponents ν_{\parallel} and ν_{\perp} are related through

$$\nu_{\perp} = \nu_{\parallel} \nu , \quad (2.29)$$

ν being the dimension of the field (2.7). To relate ν_{\parallel} to ω , we first observe that ξ_{\parallel} depends only on g_0 and the membrane size L , or its inverse $\mu = 1/L$. Writing ξ_{\parallel} as a function of the renormalized coupling g and the scale μ , we thus have

$$\begin{aligned} 0 &= \mu \frac{\partial}{\partial \mu} \xi_{\parallel}(g, \mu) \\ &= \mu \frac{\partial}{\partial \mu} \left(\frac{1}{\mu} f(g) \right) \\ &= \frac{1}{\mu} (-f(g) + \beta(g) f'(g)) , \end{aligned} \quad (2.30)$$

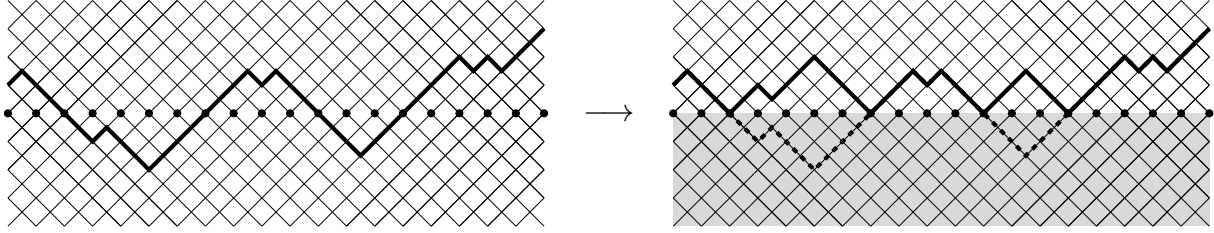


Figure 2.3: A polymer (here for simplicity directed) in interaction with a wall (thick dots). Left before and right after flapping up. The grey area is impenetrable.

where the dimension-full factor $1/\mu$ has been factored from the dependence on the dimensionless renormalized coupling g . Using that $\frac{\partial}{\partial g}\xi_{\parallel}(g) = \frac{1}{\mu}f'(g)$, this can be rewritten as

$$\begin{aligned}\xi_{\parallel}(g) &= \beta(g)\frac{\partial}{\partial g}\xi_{\parallel}(g) \\ &\approx \omega(g^*)(g - g^*)\frac{\partial}{\partial g}\xi_{\parallel}(g).\end{aligned}\quad (2.31)$$

The solution to the above equation is

$$\xi_{\parallel} \sim |g - g^*|^{1/\omega(g^*)}.\quad (2.32)$$

This leads to the identification

$$\nu_{\parallel} = -\frac{1}{\omega(g^*)}, \quad \nu_{\perp} = -\frac{\nu}{\omega(g^*)}.\quad (2.33)$$

Note that $\omega(g^*) < 0$ at the transition. Specializing to $(D, d) = (1, 1)$, we find

$$\nu_{\perp} = 1, \quad \nu_{\parallel} = 2.\quad (2.34)$$

These exponents are also valid for the delocalization transition of a 1-dimensional interface from an attractive hard wall in 2-dimensional bulk space [8,14,6]. This can be understood as follows: The partition function of a fluctuating polymer interacting with a δ -defect at the boundary of a hard wall can be written as

$$\mathcal{Z} = \frac{1}{2} \sum_{n=0}^{\infty} \mathcal{Z}_n \left(\frac{1}{2}\right)^n e^{-n\beta E},\quad (2.35)$$

where the sum runs over the number of contacts with the defect hyper-plane. E denotes the contact energy, $\beta = (k_B T)^{-1}$ and \mathcal{Z}_n is the constrained partition function of the free interface having exactly n points of contact with the defect. The powers of $\frac{1}{2}$ only appear in the presence of an impenetrable defect and reflect the fact that all configurations in the presence of a hard wall can be obtained by flapping up those parts of the polymer which have penetrated the line (see figure 2.3). This accounts for a factor $\frac{1}{2}$ for each possible flap. Thus, the hard wall constraint translates into a shift in the binding energy according to

$$E_{\text{no wall}} \longrightarrow E_{\text{wall}} = E_{\text{no wall}} + k_B T \ln 2.\quad (2.36)$$

The delocalization transition occurring for $(D, d) = (1, 1)$ at vanishing potential strength is shifted to an attractive interaction dependent on the temperature. Due to the correspondence (2.36) the exponents characterizing the transition remain unchanged.

3 Operator product expansion and one-loop result

The partition function of the model has been defined in (2.5). Analogously, we define the expectation value of an observable $\mathcal{O}(r)$ as (we denote r for \vec{r} from now on)

$$\langle \mathcal{O}(r) \rangle_{g_0} := \frac{\int \mathcal{D}[r] \exp(-\mathcal{H}[r])}{Z(g_0)}. \quad (3.1)$$

Most physical observables can be derived from expectation values of general M -point vertex operators like

$$\mathcal{O}(r) = \prod_{j=1}^M e^{ip_j r(s_j)}. \quad (3.2)$$

Before we go on, let us make some changes in normalizations which will be helpful in the following. First, we rescale the field and the coupling constant according to

$$r \longrightarrow (2-D)^{1/2} r, \quad g_0 \longrightarrow (2-D)^{d/2} g_0. \quad (3.3)$$

Second, we change the integration over internal coordinates to

$$\int_x := \frac{1}{S_D} \int \mathbf{d}^D x, \quad S_D = 2 \frac{\pi^{D/2}}{\Gamma(D/2)} \quad (3.4)$$

being the volume of the D -dimensional unit-sphere. Third, the normalization of the δ -distribution is changed to

$$\tilde{\delta}^d(r(x)) := (4\pi)^{d/2} \delta(r(x)) = \int_k e^{ikr(x)} \quad (3.5)$$

with

$$\int_k := \pi^{-d/2} \int \mathbf{d}^d k. \quad (3.6)$$

The advantage of these normalizations is that

$$\int_k e^{-k^2} = 1, \quad \int_x \Theta(|x| < 1) = 1. \quad (3.7)$$

The model in the new normalizations now reads

$$\mathcal{H}[r] = \frac{1}{2-D} \int_x \frac{1}{2} (\nabla r(x))^2 + g_0 \int_x \tilde{\delta}^d(r(x)), \quad (3.8)$$

and (due to the factor of $1/(2-D)$ in the above definition) the two-point correlator is

$$C(x_i - x_j) := \frac{1}{2d} \langle [r(x_i) - r(x_j)]^2 \rangle_0 = |x_i - x_j|^{2\nu}. \quad (3.9)$$

We now proceed with the calculation of physical observables. As an explicit example, let us consider the perturbation expansion of the 1-point vertex operator

$$\mathcal{Z}^{(p)} := \mathcal{Z}(g_0) \langle e^{ipr(s)} \rangle_{g_0} = \sum_{N=0}^{\infty} \frac{(-g_0)^N}{N!} \mathcal{Z}_N^{(p)}, \quad (3.10)$$

where

$$\mathcal{Z}_N^{(p)} = \left\langle e^{ipr(s)} \prod_{i=1}^N \int_{x_i} \tilde{\delta}^d(r(x_i)) \right\rangle_0. \quad (3.11)$$

This can be written as

$$\mathcal{Z}_N^{(p)} = \prod_{i=1}^N \int_{x_i} \int_{k_i} \tilde{\delta}^d(p + \sum k_i) \times \left\langle \exp \left[i \left(\sum_{i=1}^N k_i r(x_i) + pr(s) \right) \right] \right\rangle_0, \quad (3.12)$$

where we have already integrated out a global translation of the field r . The Gaussian average is:

$$\left\langle \exp \left[i \left(\sum_{i=1}^N k_i r(x_i) + pr(s) \right) \right] \right\rangle_0 = \exp \left[\frac{1}{2} \sum_{i,j=0}^N k_i k_j C(x_i - x_j) \right], \quad k_0 = p. \quad (3.13)$$

The $\mathcal{Z}_N^{(p)}$ in (3.11) posses short distance singularities for $N \geq 2$. In order to analyze these singularities we will use the techniques of normal ordering and operator product expansion in the sequel. In our problem the procedure of normal ordering a vertex operator $e^{ik_j r(x_j)}$ turns out to be quite simple: In any expectation value, we factorize out the contractions between the vertex operators. At one-loop order or equivalently at second order in (3.10) this means that

$$e^{ik_1 r(x_1)} e^{ik_2 r(x_2)} = :e^{i(k_1 r(x_1) + k_2 r(x_2))}: e^{k_1 k_2 C(x_1 - x_2)}. \quad (3.14)$$

This can be understood as a definition of the normal ordered product $:e^{i(k_1 r(x_1) + k_2 r(x_2))}:$. Note, that equality in the above equation is meant in the sense of operators, that is when inserted into expectation values within the free theory.

Let us now turn to an explicit derivation of the OPE of two δ -interactions, i.e. we study (3.14) for small distances $x_1 - x_2$. Since the short-distance singularities appear only in the internal contractions, the normal ordered product in the r.h.s. of (3.14) is regular for small distances $x_1 - x_2$ and thus can be expanded therein. We then project the resulting terms on the corresponding operators. For that purpose we make a change in the momentum variables according to

$$\begin{pmatrix} k_1 \\ k_2 \end{pmatrix} \longrightarrow \begin{pmatrix} \frac{k_1}{2} - k_2 \\ \frac{k_1}{2} + k_2 \end{pmatrix}. \quad (3.15)$$

In internal space we change coordinates to the center of mass system:

$$\bar{x} := \frac{1}{2}(x_1 + x_2), \quad y := x_2 - x_1. \quad (3.16)$$

Thus, the r.h.s. of (3.14) takes the form

$$\begin{aligned} & :e^{i[(\frac{k_1}{2} - k_2)r(\bar{x} - y/2) + (\frac{k_1}{2} + k_2)r(\bar{x} + y/2)]}: e^{(k_1^2/4 - k_2^2)C(y)} = \\ & :e^{ik_1 r(\bar{x})} \left(1 + ik_2 y \nabla r(\bar{x}) + ik_1 \frac{1}{2!} \frac{y^\alpha y^\beta}{4} \nabla_\alpha \nabla_\beta r(\bar{x}) - \frac{(k_2 y \nabla r(\bar{x}))^2}{2!} + \dots \right) : \times \\ & \left(1 + \frac{k_1^2}{4} C(y) + \dots \right) e^{-k_2^2 C(y)}. \end{aligned} \quad (3.17)$$

Integration over k_1, k_2 yields the OPE of $\tilde{\delta}^d(r(x_1))$ with $\tilde{\delta}^d(r(x_2))$:

$$\begin{aligned} \tilde{\delta}^d(r(\bar{x} - \frac{y}{2}))\tilde{\delta}^d(r(\bar{x} + \frac{y}{2})) &= y^{-\nu d}\tilde{\delta}^d(r(\bar{x})) - y^{-\nu d+2\nu}\frac{1}{4}\partial_r^2\tilde{\delta}^d(r(\bar{x})) \\ &\quad - y^{-\nu d-2\nu+2}\frac{1}{4D}\tilde{\delta}^d(r(\bar{x}))(\nabla r(\bar{x}))^2 \\ &\quad - y^{-\nu d+2}\frac{1}{16D}(-\Delta_r)\tilde{\delta}^d(r(\bar{x}))(\nabla r(\bar{x}))^2 \\ &\quad + y^{-\nu d+2}\frac{1}{8D}\partial_{r_i}\tilde{\delta}^d(r(\bar{x}))\Delta r_i(\bar{x}) + \dots \dots \end{aligned} \quad (3.18)$$

Restricting ourselves to the most relevant next to leading operators for internal dimension D smaller than, but close to 2, the operator product expansion reads:

$$\tilde{\delta}^d(r(\bar{x} - \frac{y}{2}))\tilde{\delta}^d(r(\bar{x} + \frac{y}{2})) = y^{-\nu d}\tilde{\delta}^d(r(\bar{x})) + \sum_{n=1}^{\infty} y^{-\nu d+n(D-2)}\frac{(-\partial_r^2)^n\tilde{\delta}^d(r(\bar{x}))}{4^n n!}. \quad (3.19)$$

The OPE-coefficient in front of the leading operator, which is the δ -interaction itself, carries the leading short distance singularity. In the following we introduce some diagrammatic notation. Denoting $\bullet := \tilde{\delta}^d(r(x))$ we abbreviate the projection of two nearby δ -interactions on the δ -interaction itself as

$$(\bullet\bullet|\bullet) = y^{-\nu d}. \quad (3.20)$$

We now analyze short-distance divergences of the perturbation expansion using the OPE in (3.18). Being interested in the leading scaling behavior, we drop all subdominant terms for $0 < D < 2$, such that we only need the leading OPE-coefficient (3.20). The integral over the relative distance in $\int_y (\bullet\bullet|\bullet)$ is logarithmically divergent for $\varepsilon=0$. In order to define a counter term we use dimensional regularization, i.e. we set $\varepsilon>0$. The integral is then UV-convergent, but IR-divergent. An IR regulator or equivalently a subtraction scale $\mu=L^{-1}$ has to be introduced to define the subtraction operation. Generally, we integrate over all distances bound by the inverse subtraction scale L . The OPE-coefficient in (3.20) then reduces to a number as

$$\langle (\bullet\bullet|\bullet) \rangle_L := \int_{|y|<L} (\bullet\bullet|\bullet) = L^\varepsilon f(\varepsilon, D). \quad (3.21)$$

Let us use the scheme of minimal subtraction (MS). The internal dimension of the membrane is fixed and (3.21) is expanded in a Laurent-series in ε , starting here at order ε^{-1} . Denoting the term of order ε^p in $\langle \bullet\bullet|\bullet \rangle_L|_{L=1}$ by $\langle \bullet\bullet|\bullet \rangle_{\varepsilon^p}$, the simple pole in (3.21) is

$$\langle (\bullet\bullet|\bullet) \rangle_{\varepsilon^{-1}} = \frac{1}{\varepsilon}. \quad (3.22)$$

Of course, in this case, due to our normalizations, this is exact.

Let us rewrite the Hamiltonian in (2.6) in terms of the renormalized dimensionless coupling g . For perturbative calculations it is custom to write

$$g_0 = gZ_g\mu^\varepsilon, \quad (3.23)$$

where Z_g is the renormalization factor, which is fixed by demanding that observables remain finite in the limit of $\varepsilon \rightarrow 0$. The Hamiltonian becomes

$$\mathcal{H}[r] = \frac{1}{2-D} \int_x \frac{1}{2} (\nabla r(x))^2 + \int_x g Z_g \mu^\varepsilon \tilde{\delta}^d(r(x)) . \quad (3.24)$$

We find to one-loop order

$$Z_g = 1 + \frac{g}{2} \langle \textcircled{\bullet\bullet} | \bullet \rangle_{\varepsilon^{-1}} + O(g^2) . \quad (3.25)$$

There is no field-renormalization since the elastic part has also to describe the manifold far away from the origin, for which the interaction term can be neglected. Formally, of course, this follows from the OPE. The renormalization group β -function is defined as

$$\beta(g) := \mu \frac{d}{d\mu} \Big|_{g_0} g , \quad (3.26)$$

from what follows together with (3.23) that

$$\beta(g) = \frac{-\varepsilon g}{1 + g \frac{\partial}{\partial g} \ln Z_g} . \quad (3.27)$$

To one-loop order we obtain from (3.27) and (3.25) as anticipated earlier

$$\beta(g) = -\varepsilon g + \frac{g^2}{2} + O(g^3) . \quad (3.28)$$

The long-distance behavior of the theory is governed by the IR-stable fixed point of the RG-flow. Fixed points are zeros of the β -function:

$$\beta(g^*) = 0 \quad \Rightarrow \quad g^* = 0 \quad \text{or} \quad g^* = 2\varepsilon . \quad (3.29)$$

In section 2.2, we had defined the correction-to-scaling exponent ω . It is obtained from the slope-function $\omega(g)$, defined as

$$\omega(g) := \frac{d}{dg} \beta(g) . \quad (3.30)$$

The correction to scaling exponent is $\omega(g)$ evaluated at the fixed points, and is found to be

$$\omega(g^*=0) = -\varepsilon , \quad \omega(g^*=2\varepsilon) = \varepsilon . \quad (3.31)$$

Of course, this result is apart from the very existence of a fixed point rather trivial, since it is determined through the leading term of the β -function, which is always $-\varepsilon g$. In order to obtain any non-trivial information from the perturbation series it is thus necessary to go beyond the leading order.

4 Two-loop calculation in a MS-scheme

4.1 Operator product expansion

Let us now continue with the calculation at the two-loop order. At each order of perturbation theory there is only one new diagram. At two-loop order this comes from three coalescing δ -interactions. Again, let us rewrite the product of the three vertex operators as its expectation value times the normal ordered product:

$$\begin{aligned} & e^{ik_1 r(x_1)} e^{ik_2 r(x_2)} e^{ik_3 r(x_3)} \\ & = :e^{i[k_1 r(x_1) + k_2 r(x_2) + k_3 r(x_3)]} : e^{k_1 k_2 C(x_1 - x_2)} e^{k_1 k_3 C(x_1 - x_3)} e^{k_2 k_3 C(x_2 - x_3)} . \end{aligned} \quad (4.1)$$

We use the following change of coordinates

$$\left. \begin{aligned} \bar{x} &:= \frac{1}{3}(x_1 + x_2 + x_3) \\ a &:= x_2 - x_1 \\ b &:= x_3 - x_2 \\ c &:= x_1 - x_3 \end{aligned} \right\} \Leftrightarrow \begin{cases} x_1 = \bar{x} + \frac{1}{3}(c - a) \\ x_2 = \bar{x} + \frac{1}{3}(a - b) \\ x_3 = \bar{x} + \frac{1}{3}(b - c) \end{cases} , . \quad (4.2)$$

As at 1-loop order, $:e^{i[k_1 r(x_1) + k_2 r(x_2) + k_3 r(x_3)]} :$ is free of divergences upon approaching the points x_i , whereas the UV-divergence comes from the factor $e^{k_1 k_2 C(x_1 - x_2)} e^{k_1 k_3 C(x_1 - x_3)} e^{k_2 k_3 C(x_2 - x_3)}$. The leading term is thus obtained upon setting $x_1 = x_2 = x_3 = \bar{x}$ in $:e^{i[k_1 r(x_1) + k_2 r(x_2) + k_3 r(x_3)]} :$, dropping the gradient terms. Further shifting $k_1 \rightarrow k_1 - k_2 - k_3$, we obtain

$$e^{ik_1 r(\bar{x})} e^{(k_1 - k_2 - k_3)k_2 C(a) + k_2 k_3 C(b) + (k_1 - k_2 - k_3)k_3 C(c)} . \quad (4.3)$$

Integrating over k_1 , k_2 and k_3 yields the final result

$$\tilde{\delta}^d(r(x_1)) \tilde{\delta}^d(r(x_2)) \tilde{\delta}^d(r(x_3)) = \left(\begin{array}{c} \bullet \\ \bullet \\ \bullet \end{array} \middle| \bullet \right) \tilde{\delta}^d(r(\bar{x})) + \left(\begin{array}{c} \bullet \\ \bullet \\ \bullet \end{array} \middle| \bullet'' \right) (-\partial_r^2) \tilde{\delta}^d(r(\bar{x})) + \dots , \quad (4.4)$$

where the OPE-coefficients are given by

$$\begin{aligned} \left(\begin{array}{c} \bullet \\ \bullet \\ \bullet \end{array} \middle| \bullet \right) &= \left[C(a)C(c) - \frac{1}{4}(C(a) + C(c) - C(b))^2 \right]^{-d/2} \\ &= \left[\frac{1}{4}(a^\nu + b^\nu + c^\nu)(b^\nu + c^\nu - a^\nu)(a^\nu + c^\nu - b^\nu)(a^\nu + b^\nu - c^\nu) \right]^{-d/2} , \end{aligned} \quad (4.5)$$

which contributes to the renormalization factor at two-loop order. The first subleading term is (denoting $\bullet'' := (-\partial_r^2) \tilde{\delta}^d(r(\bar{x}))$)

$$\left(\begin{array}{c} \bullet \\ \bullet \\ \bullet \end{array} \middle| \bullet'' \right) = -\frac{1}{4} C(a)C(b)C(c) \left[\frac{1}{4}(a^\nu + b^\nu + c^\nu)(b^\nu + c^\nu - a^\nu)(a^\nu + c^\nu - b^\nu)(a^\nu + b^\nu - c^\nu) \right]^{-d/2-1} \quad (4.6)$$

4.2 Numerical calculation in $0 < D < 2$

Let us now turn to the explicit calculation of the second order contribution to the coupling constant renormalization. To two-loop order the renormalization group Z_g -factor for the coupling constant reads

$$Z_g = 1 + \frac{g}{2} \langle \text{diagram} \rangle_{\varepsilon^{-1}} - \frac{g^2}{6} \left[\langle \text{diagram} \rangle_{\varepsilon^{-2}, \varepsilon^{-1}} - \frac{3}{2} \langle \text{diagram} \rangle_{\varepsilon^{-1}}^2 \right] + \frac{g^2}{4} \langle \text{diagram} \rangle_{\varepsilon^{-1}}^2 + O(g^3). \quad (4.7)$$

Note that this Z_g -factor can either be obtained from (2.10) and (3.23) or by expanding the perturbative series and checking that divergent contributions proportional to $\tilde{\delta}(r(x))$ cancel.

The formula is arranged such that in the brackets the second order pole in ε cancels. This is, because to leading order in $1/\varepsilon$, the two-loop diagram factorizes into two one-loop diagrams. The combinatorial factor of $3/2$ is composed of a factor of 3 for the number of possible subdivergences, and a factor of $1/2$ for the nested integration: The subdivergence in the distance say a only appears in the sector (i.e. part of the domain of integration) in which a is smallest.

Let us define:

$$I_2(D, L) := \langle \text{diagram} \rangle_L - \frac{3}{2} \langle \text{diagram} \rangle_L^2. \quad (4.8)$$

Let us already note that we will later calculate in a ‘‘massive’’ scheme in fixed dimension d . In order to use the results derived here, we keep d arbitrary instead of setting $d = d_c$. We now want to derive an expression which can be integrated numerically. Since the bounds on the integrations in (4.8) are asymmetric (remind that in $\langle \text{diagram} \rangle_L$ all 3 distances a , b , and c are bounded by L , whereas $\langle \text{diagram} \rangle_L^2$ is an integral with two bounds only) we treat both terms separately. We start with the first one, which can be written as

$$I_2^M(D, L) = \int_{a,b,c} \Theta(a \leq L) \Theta(b \leq L) \Theta(c \leq L) \left(\text{diagram} \right). \quad (4.9)$$

The divergence when integrating over the global scale is eliminated by noting that $L \frac{\partial}{\partial L} I_2(D, L) = 2\varepsilon I_2(D, L)$. There remains of course the sub-divergences, which will be subtracted later by the counter-term. Applying this procedure to (4.9), we obtain

$$2\varepsilon I_2^M(D, L) = \int_{a,b,c} \left[\delta(a - L) \Theta(b \leq L) \Theta(c \leq L) + \delta(c - L) \Theta(b \leq L) \Theta(a \leq L) + \delta(b - L) \Theta(a \leq L) \Theta(c \leq L) \right] \left(\text{diagram} \right). \quad (4.10)$$

Since the integral is symmetric in a , b , and c , we can replace it by 3 times the first term. Introducing proper normalizations, an explicit representation for the measure and factoring out the explicit L -dependence, we obtain

$$2\varepsilon I_2^M(D, L) = 3L^{2\varepsilon} \frac{S_{D-1}}{S_D} \int_{-\infty}^{\infty} dc_{\parallel} \int_0^{\infty} dc_{\perp} c_{\perp}^{D-2} \Theta(b \leq 1) \Theta(c \leq 1) \left(\text{diagram} \right) \Big|_{a=1,b,c} \quad (4.11)$$

We also have to derive an expression for the counter-term. It can be written as

$$I_2^C(D, L) = -\frac{3}{2} \int_a \int_c a^{-\nu d} c^{-\nu d} \Theta(a \leq L) \Theta(c \leq L). \quad (4.12)$$

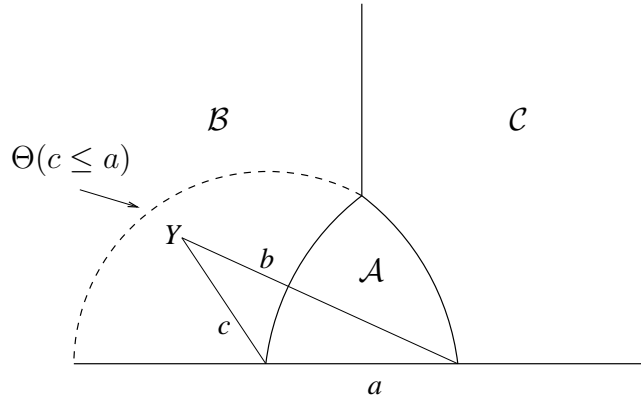


Figure 4.1: Area of integration (dashed) of the first integral in (4.13). The intersection with \mathcal{B} is to be mapped onto \mathcal{A}

Using the same trick to derive w.r.t. the IR-regulator as above, we obtain

$$2\varepsilon I_2^C(D, L) = -\frac{3}{2}L^{2\varepsilon} \int_{\mathcal{A}, \mathcal{B}, \mathcal{C}} a^{-\nu d} c^{-\nu d} \left[\delta(a-1)\Theta(c \leq a) + \delta(c-1)\Theta(a \leq c) \right]. \quad (4.13)$$

Using the technique of conformal mapping, which is presented in appendix B, both integrals above can be transformed into one having support in the single sector \mathcal{A} defined through $b, c \leq a$, (where here a is set to 1). Analogously, we define sectors \mathcal{B} and \mathcal{C} , as the subset of domains where b respectively c is the longest distance. Note that the first term in (4.13) only has contributions from \mathcal{A} and \mathcal{B} , while the second can be restricted to \mathcal{A} and \mathcal{C} after renaming a into b and c into a .

Performing explicitly the mapping of both \mathcal{B} and \mathcal{C} onto \mathcal{A} one obtains

$$\begin{aligned} \int_{\mathcal{B}} (a^{-\nu d} c^{-\nu d} \Theta(c \leq a)) \Big|_{a=1} &= \int_{\mathcal{A}} b^{-\nu d - 2\varepsilon} c^{-\nu d} \Theta(c \leq b) \\ \int_{\mathcal{C}} (a^{-\nu d} b^{-\nu d} \Theta(b \leq a)) \Big|_{a=1} &= \int_{\mathcal{A}} c^{-\nu d - 2\varepsilon} b^{-\nu d} \Theta(b \leq c). \end{aligned} \quad (4.14)$$

Combining the contributions from all sectors, we arrive at

$$2\varepsilon I_2^C(D, L) = -\frac{3}{2}L^{2\varepsilon} \int_{\mathcal{A}} (b^{-\nu d} + c^{-\nu d} + b^{-\nu d} c^{-\nu d} \max(b, c)^{-2\varepsilon}). \quad (4.15)$$

Combining (4.11) and (4.15), we obtain an expression for the complete diagram

$$\begin{aligned} 2\varepsilon I_2(D, L) &= 3L^{2\varepsilon} \frac{S_{D-1}}{S_D} \int_{-\infty}^{\infty} dc_{\parallel} \int_0^{\infty} dc_{\perp} c_{\perp}^{D-2} \Theta(b \leq 1) \Theta(c \leq 1) \\ &\times \left\{ \left[\frac{1}{4} (1+b^{\nu} + c^{\nu})(b^{\nu} + c^{\nu} - 1)(1+c^{\nu} - b^{\nu})(1+b^{\nu} - c^{\nu}) \right]^{-d/2} \right. \\ &\quad \left. - \frac{1}{2} [b^{-\nu d} + c^{-\nu d} + b^{-\nu d} c^{-\nu d} \max(b, c)^{-2\varepsilon}] \right\}. \end{aligned} \quad (4.16)$$

This expression will also be used later in a massive scheme. Since here we are only interested

in the ε -expansion, we take the limit of $\varepsilon \rightarrow 0$ in the integrand. We have made the (non-trivial) check that the integrand remains a finite integrable function, which can be integrated numerically:

$$\begin{aligned}
I_2(D, L) = & 3 \frac{L^{2\varepsilon}}{2\varepsilon} \frac{S_{D-1}}{S_D} \int_{-\infty}^{\infty} dc_{\parallel} \int_0^{\infty} dc_{\perp} c_{\perp}^{D-2} \Theta(b \leq 1) \Theta(c \leq 1) \\
& \times \left\{ \left[\frac{1}{4} (1+b^{\nu}+c^{\nu})(b^{\nu}+c^{\nu}-1)(1+c^{\nu}-b^{\nu})(1+b^{\nu}-c^{\nu}) \right]^{-d_c/2} \right. \\
& \quad \left. - \frac{1}{2} [b^{-\nu d_c} + c^{-\nu d_c} + b^{-\nu d_c} c^{-\nu d_c}] \right\} \\
& + O(\varepsilon^0). \tag{4.17}
\end{aligned}$$

Let us now proceed with the explicit numeric evaluation of (4.17). There are integrable singularities both in c_{\parallel} and c_{\perp} . To disentangle them [30,27] we make a change of variables from Cartesian coordinates $(c_{\parallel}, c_{\perp})$ to radial and angular coordinates (c, α) according to

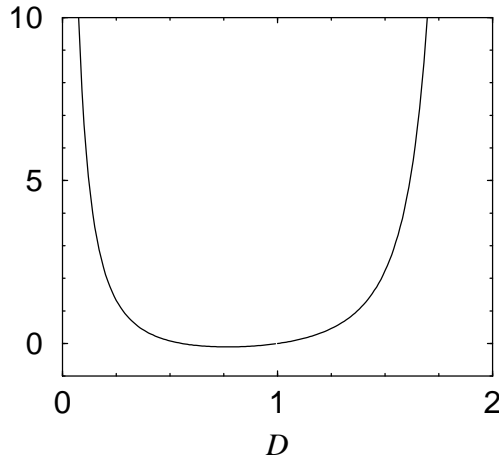
$$c_{\parallel} = c \cos(\alpha), \quad c_{\perp} = c \sin(\alpha). \tag{4.18}$$

such that

$$\int_{-\infty}^{\infty} dc_{\parallel} \int_0^{\infty} dc_{\perp} c_{\perp}^{D-2} \longrightarrow \int_0^1 dc c^{D-1} \int_0^{\pi/2} d\alpha (\sin(\alpha))^{D-2}, \tag{4.19}$$

where the upper bounds of $\pi/2$ on α and 1 on c is due to the bound of 1 on b and c . We can further restrict integration to the half-sector with $c < b$. In this sector, there remain singularities for small α and small c . The reader is invited to verify that they are eliminated by a second change of variables

$$\begin{aligned}
\alpha &= \frac{\pi}{2} \beta^{\frac{1}{D-1}} \\
c &= \tilde{c}^{\frac{1}{2-D}}.
\end{aligned}$$



D		D		D	
0.1	6.71	0.8	-0.102	1.5	2.24
0.2	2.11	0.9	-0.0712	1.6	4.45
0.3	0.847	1.0	0	1.7	10.4
0.4	0.325	1.1	0.123	1.8	36.7
0.5	0.0807	1.2	0.321	1.9	658
0.6	-0.0415	1.3	0.644	2.0	∞
0.7	-0.0949	1.4	1.20		

Figure 4.2: Numerically obtained results for the two-loop diagram in the $\overline{\text{MS}}$ -scheme. Some values are tabulated.

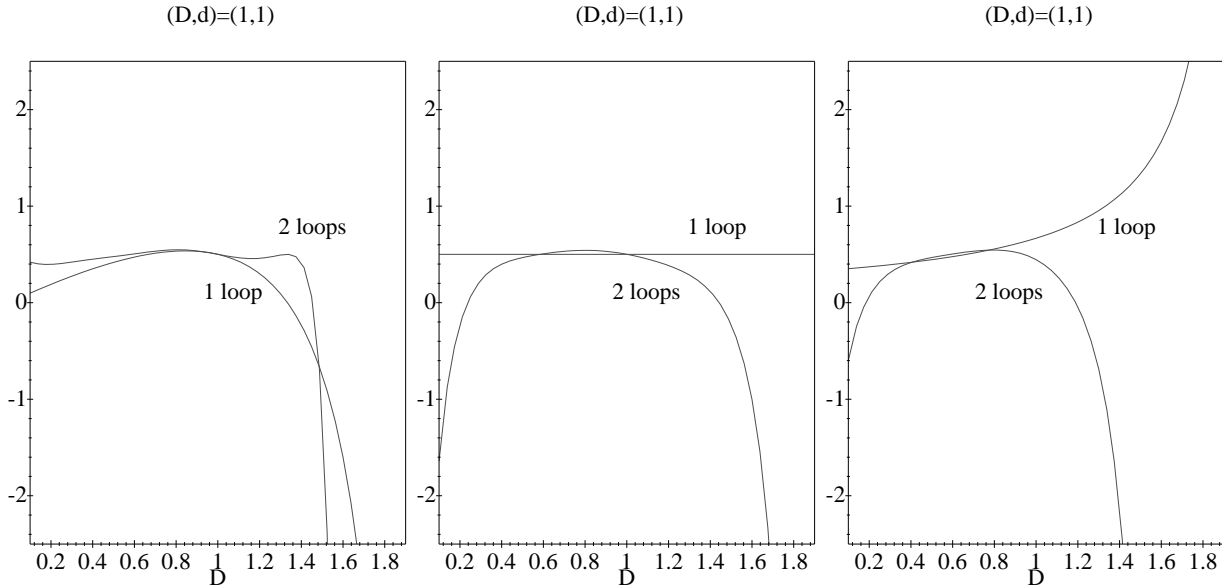


Figure 4.3: Correction to scaling exponent ω for $(D=1, d=1)$ with different extrapolation parameters (D, d) , $(D, \varepsilon(D, d))$, $(D, D_c(d))$ (from left to right). The abscissa labels the corresponding internal dimension D_0 of the departure point on the critical line $\varepsilon(D_0, d_0)=0$.

The above method works for $D > 1$ only. For $D < 1$, one has to analytically continue the integration over c_\perp in (4.11). This can be done by partial integration, since the integrand does not explicitly depend on c_\perp but on $c = \sqrt{c_\perp^2 + c_\parallel^2}$. To have no boundary terms, one should partially integrate before mapping everything onto the sector \mathcal{A} . We have explicitly checked consistency with the earlier used measure for $1 < D < 2$. Note finally, that in the special case of $D = 1$ in (4.17) the integration measure becomes a distribution reducing the integration measure to a line along c_\parallel .

The diagram is shown on figure (4.2). It grows as D^{-1} for $D \rightarrow 0$ and exponentially for $D \rightarrow 2$:

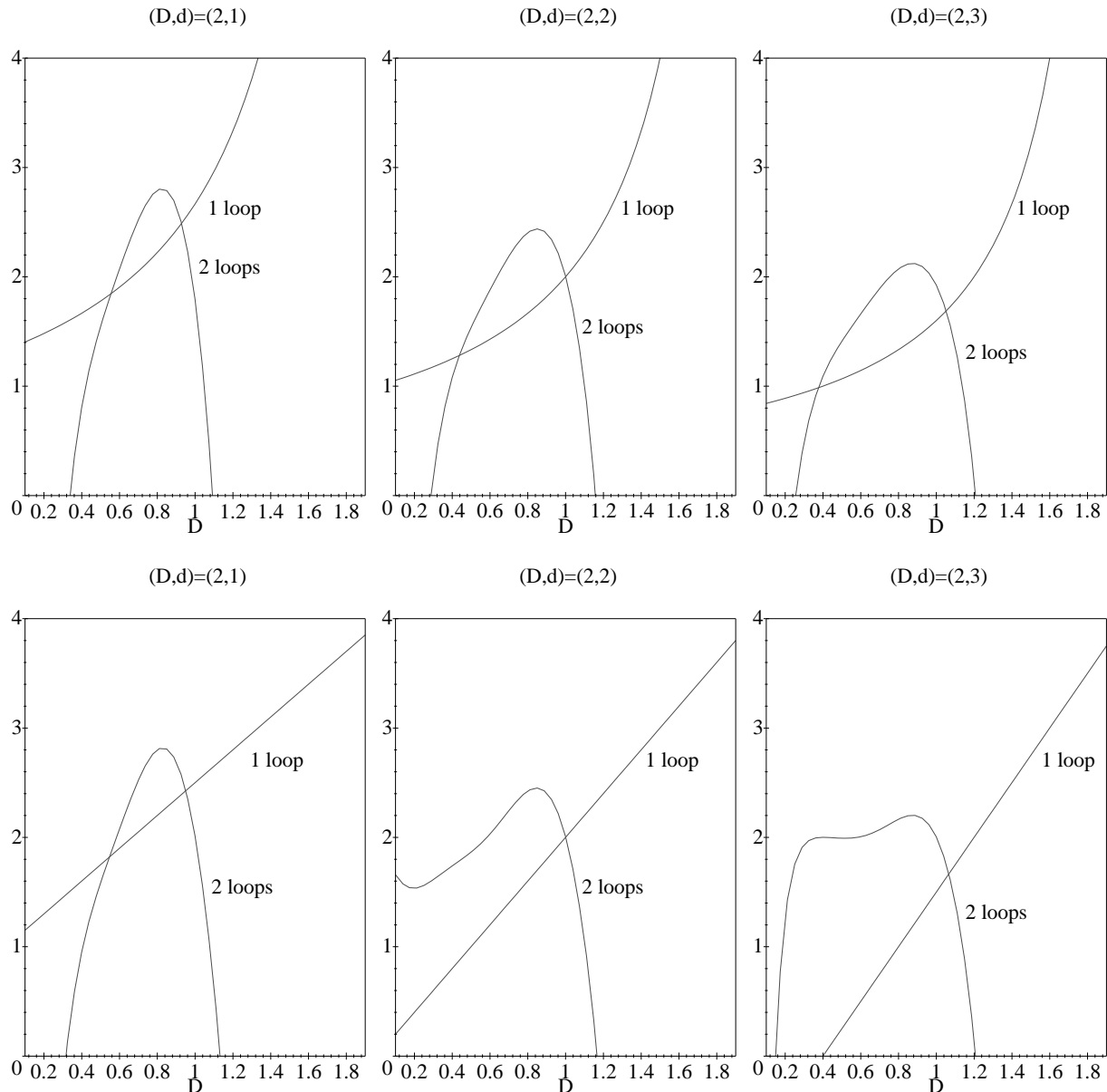
$$I_2(D) \sim \left(\frac{3}{4}\right)^{-d_c/2} \sim \left(\frac{3}{4}\right)^{-D/(2-D)}. \quad (4.20)$$

In the case of polymers $D=1$ it vanishes. The reason is that the diagrams factorize, and thus the 1-loop result is correct to all orders when working in an appropriate scheme. (See e.g. [4].)

4.3 RG-function and extrapolation

From (3.27) the renormalization β -function in second order of perturbation theory reads

$$\beta(g) = -\varepsilon g + \frac{g^2}{2} - \frac{g^3}{3} I_2(D) + O(g^4). \quad (4.21)$$



$(x, y) ; (D, d)$	(1,1)	(2,1)	(2,2)	(2,3)
$(D, D_c), \max$	0.55	2.80	2.43	2.10
$(D, d), \max$	0.55	2.80	2.43	2.20
$(D, \varepsilon), \max$	0.55			

Figure 4.4: Correction to scaling exponent ω for different extrapolation points (D, d) : Extrapolation parameters are $(D, D_c(d))$ (top) and (D, d) (bottom). The abscissa labels the corresponding internal dimension D_0 of the departure point on the critical line $\varepsilon(D_0, d_0)=0$. Furthermore, the two-loop values with minimal sensitivity with respect to the departure point are tabulated.

The long-distance behavior of the theory is governed by the IR–stable fixed point of the RG–flow. Fixed points are given by zeros of the β –function:

$$\beta(g^*) = 0 \quad \Rightarrow \quad g^* = 0 \quad \vee \quad -\varepsilon + \frac{g^*}{2} - \frac{g^{*2}}{3}I_2(D) + O(g^{*3}) = 0. \quad (4.22)$$

The physically interesting nontrivial fixed point is the one that is next to zero. In an ε –expansion it reads:

$$g^* = 2\varepsilon + \frac{8}{3}I_2(D)\varepsilon^2 + O(\varepsilon^3). \quad (4.23)$$

The correction to scaling exponent ω at this fixed point is found in an ε –expansion to be

$$\omega(g^*) = \varepsilon - \frac{4}{3}I_2(D)\varepsilon^2 + O(\varepsilon^3). \quad (4.24)$$

The question now arises of how to calculate ω for a given physical situation. The general strategy that we follow in the MS–scheme is that we make use of the freedom to choose any point on the critical line (2.2) around which to start our expansion [31,30]. To expand towards some physically interesting point (D, d) we furthermore dispose of the freedom to follow any path starting on the curve $\varepsilon=0$. Since our expansion (4.24) is exact in D but only of second order in ε , we can equally well expand it to second order in D around any point on the critical curve. Now we can change our extrapolation path through an invertible transformation $(x, y) = (x(D, d), y(D, d))$. One expresses D and ε as functions of x and y and reexpands ω to second order in x and y around the point $(x_0, y_0) = (x_0(D_0, d_c(D_0)), y_0(D_0, d_c(D_0)))$, where we recall that $d_c(D)$ is defined such that $\varepsilon(D, d_c(D)) = 0$. The aim is to find an optimal choice of variables (x, y) . The guidelines for such a choice have been discussed in [27], where this procedure has been successfully applied to extrapolate results for the anomalous dimension of self-avoiding membranes. As a general rule, we “trust” most a result that is the least sensitive to the starting point of the extrapolation. Therefore, we would like to find a plateau for some suitable chosen variables (x, y) . This procedure works well for polymers, or more generally for membranes with inner dimension close to 1. However it turns out that for membranes it works much less well than in the self-avoiding case: we could not find a plateau, but at best an extremum.

Some extrapolations are shown in the following figures (4.3, 4.4). We start with polymers interacting with a δ –wall corresponding to the point $(D, d) = (1, 1)$. (Note that for $d < 2$ the interaction becomes relevant for polymers.) This can be seen on fig. 4.3. The values obtained from the plateaus appearing at the two-loop level ($\omega \approx 0.55$) are quite close to the exact value $\omega = 1/2$, known from the fact that the result in $D = 1$ at one-loop is exact. From the latter it follows that it is best to use (D, ε) as extrapolation parameters and to stay in $D = 1$.

Let us now turn to the results obtained for ω extrapolated to points $D = 2$ (fig. 4.13): The extrapolated value depends strongly on the starting-point on the critical line. We can identify a least sensitive value, which lies below $D = 1$, reflecting the D –dependence of the two-loop diagram. We obtain identical results for different extrapolation paths. Note, that if we fix $d = 1$ and perform an ε –expansion in D as is commonly done [32], then, this corresponds to starting from $D_c(d=1) = 2/3 < 1$. The d –dependence of the extrapolated values is recovered in the massive scheme, which we discuss in the next section.

5 Calculation in fixed dimension: The massive scheme

5.1 Phantom manifolds

An alternative scheme to an ε -expansion is a calculation in fixed dimension. This way we hope to circumvent the difficulty that we faced when calculating the two-loop diagram in the previous section in the limit of $D \rightarrow 2$: Since the diagram behaves like $(\frac{4}{3})^{d/2}$, it becomes large when the dimension of the embedding space is large. When working in an ε -expansion, d and D are related by $\varepsilon = D - d(2 - D)/2$ and sending $\varepsilon \rightarrow 0$ before $D \rightarrow 2$ imposes that $d \rightarrow \infty$. Thus one would like to work at finite d , thus finite ε . The diagrams are UV-convergent for $d < d_c$. They are cut-off in the infrared by a finite membrane size. Alternatively, we can use a “soft” IR cut-off, that is we introduce a chemical potential τ into the Hamiltonian and sum over all manifold sizes. For polymers ($D = 1$) this scheme corresponds to a “massive scheme” in an $O(N)$ -symmetric, scalar ϕ^4 -theory as can be seen via a de Gennes Laplace transformation on the $N = 0$ component limit. (The correlator in momentum-space reads $\frac{1}{k^2 + t}$) In the following we keep a hard IR regulator and calculate the two-loop diagram in fixed dimension. We use the analytical expression given in (4.16). For the numerical integration in $1 < D < 2$ we proceed as before. The result for different embedding dimensions d is shown graphically on figure 5.1, where also some explicit values in the limit of $D = 2$ are given. Note, that the exact factorization-property in the limit of $D = 1$ is only valid in the MS-scheme or in a massive scheme with suitable soft cut-off as mentioned above. However, even the method is not tailored to capture that feature, the obtained value $\omega = 0.6$ in the case of $(D, d) = (1, 1)$ is not too far from the exact value $1/2$. We expect that higher order terms would again reproduce the exact value of $\omega = 1/2$. Also note that results for membranes ($D = 2$) are close to those from the ε -expansion, especially for small d .

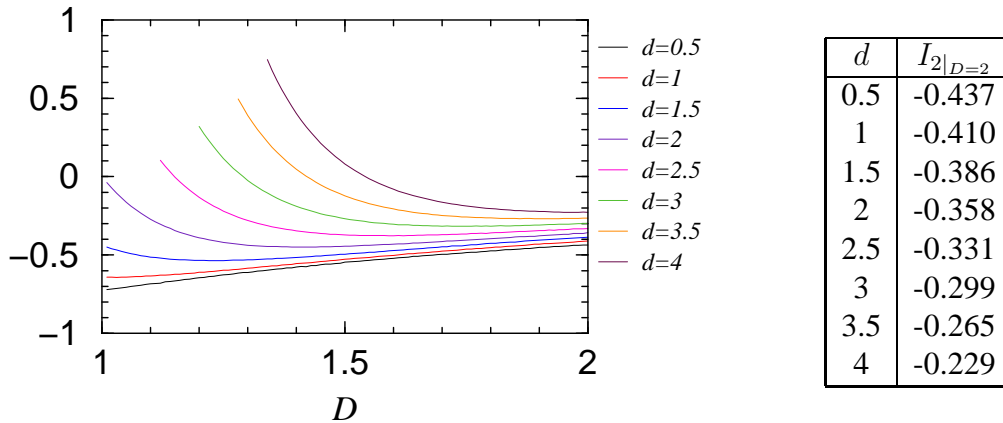


Figure 5.1: 2-loop diagram in fixed dimension for embedding dimensions $d=0.5$ to $d=4$ (from bottom to top). The curves are only shown for values of D such that $\varepsilon \geq 0$.

5.2 Self-avoiding membranes

Up to now we were considering a D -dimensional polymerized “phantom” membrane interacting with a point-like impurity in d -dimensional embedding space modeled through a δ -potential.

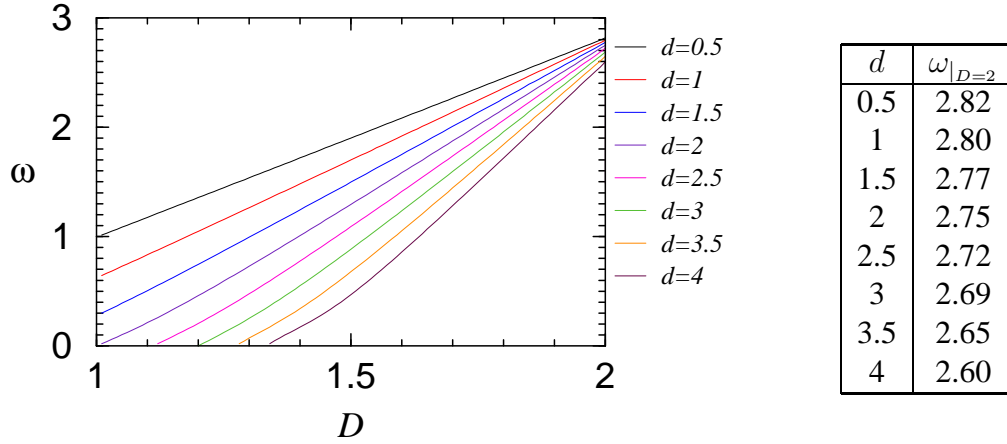


Figure 5.2: Correction to scaling exponent ω for embedding dimension $d=0.5$ to $d=4$ (from top to bottom). ε is restricted to $\varepsilon \geq 0$; otherwise one has to work with an explicit UV-cutoff.

The infinite fractal dimension of the free manifold was causing problems, and since all operators of the type $(-\Delta_r)^n \delta(r)$, $n \geq 0$, attain the same relevance in $D = 2$, it is not clear whether the model will break down. Physically, the problem is much better defined for self-avoiding membranes. From field-theoretical calculations, which have recently been refined up to two-loop [26,27], we know that two-dimensional self-avoiding manifolds embedded in three dimensional space have an anomalous dimension of $\nu^* \approx 0.85$. We now try to overcome the problem of an infinite Hausdorff-dimension by a crude simplification: We approximate the self-avoiding manifold by a Gaussian theory with the same scaling dimension, that is a Hamiltonian of the type [16]

$$\mathcal{H}[r] = \frac{1}{k-D} \int_x \frac{1}{2} r(x) (-\Delta_x)^{k/2} r(x), \quad (5.1)$$

where

$$r : x \in \mathbb{R}^D \longrightarrow r(x) \in \mathbb{R}^d$$

as before providing the two-point correlator in our normalizations:

$$C(x, y) = |x-y|^{k-D}. \quad (5.2)$$

The scaling dimension is

$$\nu = \frac{k-D}{2}. \quad (5.3)$$

We recover (3.9) by setting $k = 2$, but the model can be continued analytically to any real value of k , with $k \geq 2$. Setting

$$k^* = 2\nu^* + D \quad (5.4)$$

we get a Gaussian manifold with identical scaling dimension as obtained for self-avoiding crumpled membranes at two-loop. The critical embedding dimension of the interaction then reads

$$d_c = \frac{2D}{k^* - D} = \frac{D}{\nu^*}, \quad (5.5)$$

that is the interacting is relevant in $d < d_c$. For membranes $d_c = \frac{2}{0.85} \approx 2.4$. All operators of the type $(-\Delta_r)^n \delta^d(r)$ are at least naively irrelevant for $n > 0$, as

$$[(-\Delta_r)^n \delta^d(r)] = -\nu^*(d + 2n) \quad (5.6)$$

and the corresponding coupling has in inverse length units the dimension

$$[g_0^{(n)}] = D - \nu^*(d + 2n) < 0, \quad n > 0. \quad (5.7)$$

We may repeat the calculation in the massive scheme setting the free scaling dimension $\nu^*=0.85$ and $(D, d)=(2, 1)$. The result is shown in table (5.2).

Let us stress that this method can not be turned into a systematic expansion, since perturbation theory neglects all effects of the non-Gaussian nature of the nontrivial crumpled state. We only know that for $d \rightarrow \infty$ the Gaussian variational approximation for the Hamiltonian, i.e. (5.1) becomes exact [33–35].

	I	$\omega(g^*)$	$\theta(g^*)$
1-loop	1.000	1.15	2.71
2-loop	-0.379	1.49	3.10

Table 5.1: Two-loop results for self-avoiding membranes ($D=2$) approximated through a Gaussian theory having identical scaling dimension $\nu^*=0.85$. Results are shown for the corresponding diagram, the correction to scaling exponent ω and the contact exponent θ .

6 Summation of the perturbation series in the limit $D = 2$

In the last section we introduced a “massive” scheme allowing to perform the renormalization procedure in fixed dimension. As can be seen in figures 5.1 and 5.2, the limit $D \rightarrow 2$ can be taken in the 2-loop diagram and is smooth. Surprisingly, this limit can be calculated analytically: Setting $\nu = 0$ in (4.16), the integrand becomes constant, and thus trivial to calculate. This is a striking property. Even more, if we slightly modify the regularization prescription, this property holds to *all loop orders* in perturbation theory. Below, we will give an analytic expression for the complete perturbation series, which allows for analyzing the strong coupling limit. Furthermore, we show how corrections in $(2 - D)$ can be incorporated. We will see that only the latter depend on the explicit cut-off procedure, a point which will be further clarified below. As a non-trivial check, when extrapolating back to polymers ($D = 1$), the corresponding result for ω is approximately reproduced.

6.1 N -loop order

In order to calculate the N -loop contribution to the perturbation theory we need the SDE of $N + 1$ contact interactions. The normal ordered product of the corresponding vertex operators reads

$$e^{ik_1 r(x_1)} e^{ik_2 r(x_2)} \dots e^{ik_{N+1} r(x_{N+1})} = :e^{i(\sum_{n=1}^{N+1} k_n r(x_n))}: \prod_{i,j=1}^{N+1} e^{\frac{1}{2} k_i k_j C(x_i - x_j)}. \quad (6.1)$$

We choose x_{N+1} as root in the renormalization procedure (for the precise definition, see below) and therefore k_{N+1} to integrate over in order to obtain the δ -distribution (or its derivative), onto

which to project. We thus shift

$$k_{N+1} \longrightarrow k_{N+1} - \sum_{j=1}^N k_j$$

and rewrite the quadratic form in (6.1) as

$$\begin{aligned} \frac{1}{2} \sum_{i,j=1}^{N+1} k_i k_j C(x_i - x_j) &= \sum_{j=1}^N k_{N+1} k_j C(x_{N+1} - x_j) + \frac{1}{2} \sum_{i,j=1}^N k_i k_j C(x_i - x_j) \\ &\longrightarrow \sum_{j=1}^N k_{N+1} k_j C(x_{N+1} - x_j) - \sum_{i,j=1}^N k_i k_j C(x_{N+1} - x_j) + \frac{1}{2} \sum_{i,j=1}^N k_i k_j C(x_i - x_j) \\ &= \sum_{j=1}^N k_{N+1} k_j C(x_{N+1} - x_j) - \sum_{i,j=1}^N k_i k_j \frac{C(x_{N+1} - x_i) + C(x_{N+1} - x_j) - C(x_i - x_j)}{2}. \end{aligned} \quad (6.2)$$

(6.1) then becomes (up to subdominant terms¹ involving spatial derivatives of r)

$$\begin{aligned} &:\exp [ik_{N+1}r(x_{N+1})]: \\ &\times \exp \left[\sum_{j=1}^N k_{N+1} k_j C(x_{N+1} - x_j) - \sum_{i,j=1}^N k_i k_j \frac{C(x_{N+1} - x_i) + C(x_{N+1} - x_j) - C(x_i - x_j)}{2} \right] \end{aligned} \quad (6.3)$$

and the integration over k_{N+1} produces the δ -interaction and its derivatives; the latter come from the first term in (6.2). They are subdominant and thus will be dropped. We abbreviate the quadratic form in (6.2) as (D_{ij}) , where the matrix elements are

$$\begin{aligned} D_{ij} &= \frac{1}{2} [C(x_{N+1} - x_i) + C(x_{N+1} - x_j) - C(x_i - x_j)], \quad i \neq j, \\ D_{ii} &= C(x_{N+1} - x_i). \end{aligned} \quad (6.4)$$

Integrating out the momenta k_1, \dots, k_N yields the operator product expansion of $N + 1$ contact interactions as

$$\begin{aligned} \tilde{\delta}^d(r(x_1)) \tilde{\delta}^d(r(x_2)) \dots \tilde{\delta}^d(r(x_{N+1})) &= [\det(D_{ij})]^{-d/2} \tilde{\delta}^d(r(x_{N+1})) \\ &\quad + \text{subdominant operators}. \end{aligned} \quad (6.5)$$

6.2 The limit $D \rightarrow 2$ and $(2-D)$ -expansion

Whereas (6.5) is still completely general, we now want to study the limit $D \rightarrow 2$ as well as perturbations above it. We start by remarking that the matrix (D_{ij}) may be expanded in powers of $2-D$:

$$D_{ij} = \sum_{n=0}^{\infty} \frac{(2-D)^n}{n!} D_{ij}^{(n)}, \quad (6.6)$$

¹Here we argue in terms of an OPE. Note that in order to make these arguments rigorous, one should ask of whether these terms affect the effective action at *constant* background-field. This is not the case, since then $\nabla r = 0$.

where

$$\begin{aligned} D_{ij}^{(n)} &= \frac{\mu^{-2\nu}}{2} (\ln^n |(x_{N+1}-x_i)\mu| + \ln^n |(x_{N+1}-x_j)\mu| - \ln^n |(x_i-x_j)\mu|), \quad i \neq j \\ D_{ii}^{(n)} &= \mu^{-2\nu} \ln^n |(x_{N+1}-x_i)\mu|, \end{aligned} \quad (6.7)$$

$\mu = 1/L$. Then,

$$\begin{aligned} \det(D) &= \exp[\text{Tr} \ln(D_{ij})] \\ &= \det(D^{(0)}) \cdot \exp[\text{Tr} \ln[\mathbf{1} + \sum_{n=1}^{\infty} \frac{(2-D)^n}{n!} [D^{(0)}]^{-1} D^{(n)}]], \end{aligned} \quad (6.8)$$

where $[D^{(0)}]^{-1}$ denotes the inverse matrix to $D^{(0)}$. Let us expand the OPE-coefficient in (6.5) up to second order in $2 - D$. Expanding first the logarithm,

$$\begin{aligned} \ln[\mathbf{1} + \sum_{n=1}^{\infty} \frac{(2-D)^n}{n!} [D^{(0)}]^{-1} D^{(n)}] \\ = (2-D)[D^{(0)}]^{-1} D^{(1)} + \frac{(2-D)^2}{2} [[D^{(0)}]^{-1} D^{(2)} - ([D^{(0)}]^{-1} D^{(1)})^2] + O((2-D)^3), \end{aligned}$$

and inserting into (6.8) one arrives at

$$\begin{aligned} [\det(D)]^{-d/2} &= [\det(D^{(0)})]^{-d/2} \left[1 - \frac{(2-D)d}{2} \text{Tr}[D^{(0)}]^{-1} D^{(1)} \right. \\ &\quad \left. - \frac{(2-D)^2 d}{4} \left[\text{Tr}[D^{(0)}]^{-1} D^{(2)} - \text{Tr}([D^{(0)}]^{-1} D^{(1)})^2 - \frac{d}{2} \text{Tr}^2[D^{(0)}]^{-1} D^{(1)} \right] + O((2-D)^3) \right]. \end{aligned} \quad (6.9)$$

The zeroth order is $[\det(D^{(0)})]^{-d/2}$. In order to proceed we need the latter and the inverse matrix $[D^{(0)}]^{-1}$. Let us first calculate the determinant. From (6.6) we have

$$\begin{aligned} D^{(0)} &= \mu^{-2\nu} \begin{pmatrix} 1 & \frac{1}{2} & \cdots & \frac{1}{2} \\ \frac{1}{2} & 1 & \ddots & \vdots \\ \vdots & \ddots & \ddots & \frac{1}{2} \\ \frac{1}{2} & \cdots & \frac{1}{2} & 1 \end{pmatrix} = \frac{\mu^{-2\nu}}{2} \left(\begin{pmatrix} 1 & \cdots & 0 \\ \vdots & \ddots & \vdots \\ 0 & \vdots & 1 \end{pmatrix} + \begin{pmatrix} 1 & \cdots & 1 \\ \vdots & \ddots & \vdots \\ 1 & \cdots & 1 \end{pmatrix} \right) = \frac{\mu^{-2\nu}}{2} (\mathbf{1} + N\mathbf{P}), \\ \mathbf{P} &= \frac{1}{N} \begin{pmatrix} 1 & \cdots & 1 \\ \vdots & \ddots & \vdots \\ 1 & \cdots & 1 \end{pmatrix} \end{aligned} \quad (6.10)$$

being the projector onto $(1, 1, \dots, 1)$. Denoting by $\dim \text{Im}(\mathbf{P})$ the dimension of the space onto which \mathbf{P} projects one has the general formula:

$$\det(\mathbf{1} + a\mathbf{P}) = (1 + a)^{\dim \text{Im}(\mathbf{P})}.$$

Since here $\dim \text{Im}(\mathbf{P}) = 1$, we find

$$\det(D^{(0)}) = \mu^{-2\nu N} \frac{1 + N}{2^N}. \quad (6.11)$$

The inverse matrix of $(\mathbf{1} + N\mathbf{P})$ can be inferred from the ansatz

$$(\mathbf{1} + N\mathbf{P})(\mathbf{1} + b\mathbf{P}) = \mathbf{1} .$$

Since \mathbf{P} is a projector $\mathbf{P}^2 = \mathbf{P}$ and this implies

$$(N + b + Nb) \mathbf{P} = \mathbf{0} .$$

Therefore, $b = -N/(N + 1)$ and

$$[D^{(0)}]^{-1} = 2 \left(\mathbf{1} - \frac{N}{N+1} \mathbf{P} \right) \mu^{2\nu} . \quad (6.12)$$

To obtain the first order contribution in $(2-D)$ from eq. (6.8) we only need $[D^{(0)}]^{-1}D^{(1)}$, which reads

$$([D^{(0)}]^{-1}D^{(1)})_{ij} = \left(2D_{ij}^{(1)} - \frac{2}{1+N} \sum_{k=1}^N D_{ik}^{(1)} \right) \mu^{2\nu} . \quad (6.13)$$

The trace of (6.13) can easily be performed, with the result

$$\text{Tr}([D^{(0)}]^{-1}D^{(1)}) = \left(\frac{2N}{1+N} \sum_{i=1}^N D_{ii}^{(1)} - \frac{2}{1+N} \sum_{i=1}^N \sum_{k=1}^N (1 - \delta_{ik}) D_{ik}^{(1)} \right) \mu^{2\nu} . \quad (6.14)$$

In order to factorize the integrals as much as possible, we found it convenient to modify the regularization prescription (3.21). In each order of perturbation theory we have to integrate the expression (6.5) over internal distances. These integrals have to be regularized in the infrared through an appropriate IR cut-off. In the preceding sections we have cut off the integrals such that all relative distances between internal points were smaller than $L = 1/\mu$. In the following we replace this by the demand that all distances from the fixed, but arbitrarily chosen point x_{N+1} , the root of the subtraction prescription, are bounded by L . Other distances are not restricted (see fig. 6.1). Alternatively, one could calculate on a closed manifold of finite size. Of course, then the correlator has to be modified. Work is in progress to implement this procedure, which has the advantage of being more systematic [29].

To simplify the calculations, we further introduce the following notation:

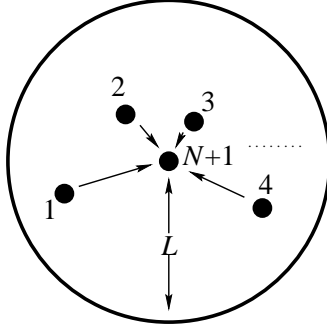
$$\overline{f(x_{i_1}, \dots, x_{i_k})} := \int_{x_1} \cdots \int_{x_N} f(x_{i_1}, \dots, x_{i_k}) \quad (6.15)$$

with new normalization

$$\int_x := \frac{D}{S_D} \int \mathbf{d}^D x \theta(|x| < 1) , \quad (6.16)$$

which is chosen such that the overbar can be thought of as an averaging procedure, and especially

$$\overline{1} = 1 . \quad (6.17)$$

Figure 6.1: Regularization scheme for the N -loop diagrams

Thanks to our regularization prescription the integral of (6.14) over internal points can be replaced by μ^{-ND} (for the integration measure L^{ND}) times

$$\begin{aligned} \overline{\text{Tr}([D^{(0)}]^{-1}D^{(1)})} &= \frac{2N^2}{1+N} \overline{\ln |(x_{N+1} - x_i)|} \\ &\quad - \left(\frac{2N(N-1)}{1+N} \right) \left(\overline{\ln |x_{N+1} - x_i|} - \frac{1}{2} \overline{\ln |x_i - x_j|} \right) \\ &= \frac{2N}{1+N} \overline{\ln |x_{N+1} - x_i|} + \frac{N(N-1)}{1+N} \overline{\ln |x_i - x_j|}, \end{aligned} \quad (6.18)$$

Introducing a diagrammatic notation

$$\begin{array}{c} \text{N+1} \\ \circlearrowleft \\ i \end{array} := \overline{\ln |x_{N+1} - x_i|} \quad (6.19)$$

and

$$\begin{array}{c} \text{N+1} \\ \circlearrowleft \\ i \quad j \end{array} := \overline{\ln |x_j - x_i|}, \quad (6.20)$$

the N -loop integral reads up to first order in $2-D$

$$\begin{aligned} \int (\det D)^{-d/2} &= \mu^{-N\epsilon} \left(\frac{1+N}{2^N} \right)^{-d/2} \times \left[1 - \frac{d}{2}(2-D) \left(\frac{2N}{1+N} \begin{array}{c} \text{N+1} \\ \circlearrowleft \\ i \end{array} + \frac{N(N-1)}{1+N} \begin{array}{c} \text{N+1} \\ \circlearrowleft \\ i \quad j \end{array} \right) \right. \\ &\quad \left. + O((2-D)^2) \right]. \end{aligned} \quad (6.21)$$

We now turn to an explicit calculation of the diagrams. To first order in $2-D$ we have two contributions. The first (6.19) is

$$\begin{array}{c} \text{N+1} \\ \circlearrowleft \\ i \end{array} = \int_{x_i} \ln |x_{N+1} - x_i| = D \int_0^1 \frac{dx x^D}{x} \ln x = -\frac{1}{D} \rightarrow -\frac{1}{2}, \quad \text{as } D \rightarrow 2. \quad (6.22)$$

The second diagram (6.20) is

$$\begin{array}{c} \text{N+1} \\ \circlearrowleft \\ i \quad j \end{array} = \frac{D^2}{S_D^2} \int_0^1 d^D x_i d^D x_j \ln |\vec{x}_i - \vec{x}_j|,$$

where we have put vectors to stress that $x_i - x_j$ is not a scalar. It suffices to evaluate this in $D = 2$. We find

$$\textcircled{i \dots j}^{N+1} = -\frac{1}{4}. \quad (6.23)$$

Combining (6.21), (6.22) and (6.23) we finally obtain for the renormalized coupling g up to first order in $2 - D$:

$$\begin{aligned} g &= g_0 \mu^{-\varepsilon} \left(1 + \sum_{N=1}^{\infty} \frac{(-g_0 2^{d/2} \mu^{-\varepsilon})^N}{(N+1)!(1+N)^{d/2}} \times \right. \\ &\quad \left. \times \left[1 - (2-D) \frac{d}{2} \left(\frac{2N}{1+N} \textcircled{i \dots j}^{N+1} + \frac{N(N-1)}{1+N} \textcircled{i \dots j}^{N+1} \right) + \dots \right] \right) \\ &= g_0 \mu^{-\varepsilon} \left(1 + \sum_{N=1}^{\infty} \frac{(-g_0 2^{d/2} \mu^{-\varepsilon})^N}{(N+1)!(1+N)^{d/2}} \left[1 + (2-D) \frac{d}{2} \left(\frac{N}{1+N} + \frac{N(N-1)}{4(1+N)} \right) + \dots \right] \right) \end{aligned} \quad (6.24)$$

This can also be written as

$$\begin{aligned} g 2^{d/2} &= - \sum_{N=1}^{\infty} \frac{(-g_0 2^{d/2} \mu^{-\varepsilon})^N}{N! N^{d/2}} \\ &\quad - (2-D) \frac{d}{2} \sum_{N=1}^{\infty} \frac{(-g_0 2^{d/2} \mu^{-\varepsilon})^N (N-1)}{N! N^{d/2+1}} \\ &\quad - (2-D) \frac{d}{8} \sum_{N=1}^{\infty} \frac{(-g_0 2^{d/2} \mu^{-\varepsilon})^N (N-1)(N-2)}{N! N^{d/2+1}}. \end{aligned} \quad (6.25)$$

Absorbing a factor of $2^{d/2}$ both in g and g_0 and defining the dimensionless coupling $z := g_0 \mu^{-\varepsilon}$, we obtain the final result

$$\begin{aligned} g &= - \sum_{N=1}^{\infty} \frac{(-z)^N}{N! N^{d/2}} - (2-D) \frac{d}{2} \sum_{N=1}^{\infty} \frac{(-z)^N (N-1)}{N! N^{d/2+1}} - (2-D) \frac{d}{8} \sum_{N=1}^{\infty} \frac{(-z)^N (N-1)(N-2)}{N! N^{d/2+1}} \\ &\quad + O(2-D)^2. \end{aligned} \quad (6.26)$$

This formula is the starting point for further analysis in the subsequent sections.

6.3 Asymptotic behavior of the series

In the following we are interested in the limit of large z (strong repulsion), which also is the scaling behavior of infinitely large membranes. We therefore need an analytical expression for sums like (6.26) in the limit of large z . An example is the leading order expression

$$g = - \sum_{N=1}^{\infty} \frac{(-z)^N}{N! N^{d/2}}. \quad (6.27)$$

²The expression in parenthesis is the inverse renormalization Z_g -factor which relates the bare coupling g_0 to the renormalized coupling g according to $g Z_g \mu^\varepsilon = g_0$.

For the following analysis we need an integral representation of the above series. We claim that for all $k, d > 0$

$$\sum_{N=0}^{\infty} \frac{(-z)^N}{N!(k+N)^{d/2}} = \frac{1}{\Gamma(\frac{d}{2})} \int_0^{\infty} dr r^{d/2-1} \exp[-z e^{-r} - kr] . \quad (6.28)$$

This can be proven as follows:

$$\begin{aligned} \frac{1}{\Gamma(\frac{d}{2})} \int_0^{\infty} dr r^{d/2-1} \exp[-z e^{-r} - kr] &= \frac{1}{\Gamma(\frac{d}{2})} \sum_{N=0}^{\infty} \frac{(-z)^N}{N!} \int_0^{\infty} dr r^{d/2-1} e^{-(N+k)r} \\ &= \frac{1}{\Gamma(\frac{d}{2})} \sum_{N=0}^{\infty} \frac{(-z)^N}{N!} \frac{\Gamma(\frac{d}{2})}{(N+k)^{d/2}} . \end{aligned}$$

This integral-representation is not the most practical for our purpose. It is better to set $r \rightarrow s := e^{-r}$ which yields

$$\sum_{N=0}^{\infty} \frac{(-z)^N}{N!(k+N)^{d/2}} = \frac{1}{\Gamma(\frac{d}{2})} \int_0^1 ds s^{k-1} (-\ln s)^{d/2-1} e^{-sz} . \quad (6.29)$$

This formula is already very useful for some purposes. It is still advantageous to make a second variable-transformation $s \rightarrow y := sz$, yielding

$$\sum_{N=0}^{\infty} \frac{(-z)^N}{N!(k+N)^{d/2}} = \frac{(\ln z)^{d/2-1}}{\Gamma(\frac{d}{2}) z^k} \int_0^z dy y^{k-1} \left(1 - \frac{\ln y}{\ln z}\right)^{d/2-1} e^{-y} . \quad (6.30)$$

Finally we remark that we usually have the following combination

$$f_k^d(z) := z^k \sum_{N=0}^{\infty} \frac{(-z)^N}{N!(k+N)^{d/2}} = \frac{(\ln z)^{d/2-1}}{\Gamma(\frac{d}{2})} \int_0^z dy y^{k-1} \left(1 - \frac{\ln y}{\ln z}\right)^{d/2-1} e^{-y} . \quad (6.31)$$

It satisfies the following simple recursion relation, which is helpful to calculate the β -function:

$$z \frac{d}{dz} f_k^d(z) = f_k^{d-2}(z) . \quad (6.32)$$

From (6.28) $f_k(z) > 0$ for all $k, d > 0$ and the behavior for large z is obtained by expanding $(1 - \frac{\ln y}{\ln z})^{d/2-1}$ for small $\frac{1}{\ln z}$

$$\begin{aligned} f_k^d(z) &= \frac{(\ln z)^{d/2-1}}{\Gamma(\frac{d}{2})} \left[\int_0^{\infty} dy y^{k-1} e^{-y} \right. \\ &\quad \left. - \frac{1}{\ln z} \left(\frac{d}{2} - 1\right) \int_0^{\infty} dy y^{k-1} \ln y e^{-y} \right. \\ &\quad \left. + O\left(\frac{1}{(\ln z)^2}\right) \right] \\ &\quad + O(e^{-z}) . \end{aligned} \quad (6.33)$$

The result is

$$f_k^d(z) = \frac{(\ln z)^{d/2-1} \Gamma(k)}{\Gamma(\frac{d}{2})} \left(1 - \frac{1}{\ln z} \frac{d-2}{2} \frac{\Gamma'(k)}{\Gamma(k)} + \dots \right). \quad (6.34)$$

For later reference, we note a list of useful formulas ($\gamma = 0.577216\dots$ is the Euler-constant)

$$f_1^d(z) = \frac{(\ln z)^{d/2-1}}{\Gamma(\frac{d}{2})} + \frac{\gamma(\ln z)^{d/2-2}}{\Gamma(\frac{d-2}{2})} + \frac{(6\gamma^2 + \pi^2)(\ln z)^{d/2-3}}{12\Gamma(\frac{d-4}{2})} + \dots \quad (6.35)$$

$$f_2^d(z) = \frac{(\ln z)^{d/2-1}}{\Gamma(\frac{d}{2})} + \frac{(\gamma-1)(\ln z)^{d/2-2}}{\Gamma(\frac{d-2}{2})} + \frac{(6\gamma(\gamma-2) + \pi^2)(\ln z)^{d/2-3}}{12\Gamma(\frac{d-4}{2})} + \dots \quad (6.36)$$

$$f_3^d(z) = \frac{2(\ln z)^{d/2-1}}{\Gamma(\frac{d}{2})} + \frac{(2\gamma-3)(\ln z)^{d/2-2}}{\Gamma(\frac{d-2}{2})} + \frac{(6\gamma^2 - 18\gamma + 6 + \pi^2)(\ln z)^{d/2-3}}{6\Gamma(\frac{d-4}{2})} + \dots \quad (6.37)$$

Note that with the above notations, the relation (6.26) expressing g as a function of z becomes

$$g(z) = f_1^{d+2}(z) - (2-D) \frac{d}{2} f_2^{d+4}(z) + (2-D) \frac{d}{8} f_3^{d+4}(z) + O(2-D)^2. \quad (6.38)$$

In the next two sections we shall present two formalisms which give results for ω at next to leading order. It will turn out that the results catch qualitatively correctly the cross-over to $D = 1$; however they differ in the numerical values. This is a reflection of the fact that the $(2-D)$ -expansion is not systematic. We expect that working on a manifold of finite size and using the exact correlation function on this manifold would lead to a systematic expansion. Work is in progress [29] to check this hypothesis.

6.4 The RG-functions in the bare coupling

The renormalization group β -function is defined as

$$\beta(g) := \mu \frac{d}{d\mu} \Big|_0 g. \quad (6.39)$$

Since it is hard to invert the function $g(z)$, it is advantageous to study β as function of the bare coupling z

$$\beta(g) \equiv \beta(z) = -\varepsilon z \frac{d}{dz} g. \quad (6.40)$$

To first order in $2-D$, we find from (6.38) using (6.32)

$$\beta(z) = -\varepsilon \left[f_1^d(z) + (2-D) \left(-\frac{d}{2} f_2^{d+2}(z) + \frac{d}{8} f_3^{d+2}(z) \right) + O(2-D)^2 \right]. \quad (6.41)$$

Inserting the asymptotic expansions from the last section, this becomes

$$\beta(z) = -\frac{\varepsilon}{\Gamma(\frac{d}{2})} \left[(\ln z)^{d/2-1} - \frac{2-D}{2} (\ln z)^{d/2} + \dots \right], \quad (6.42)$$

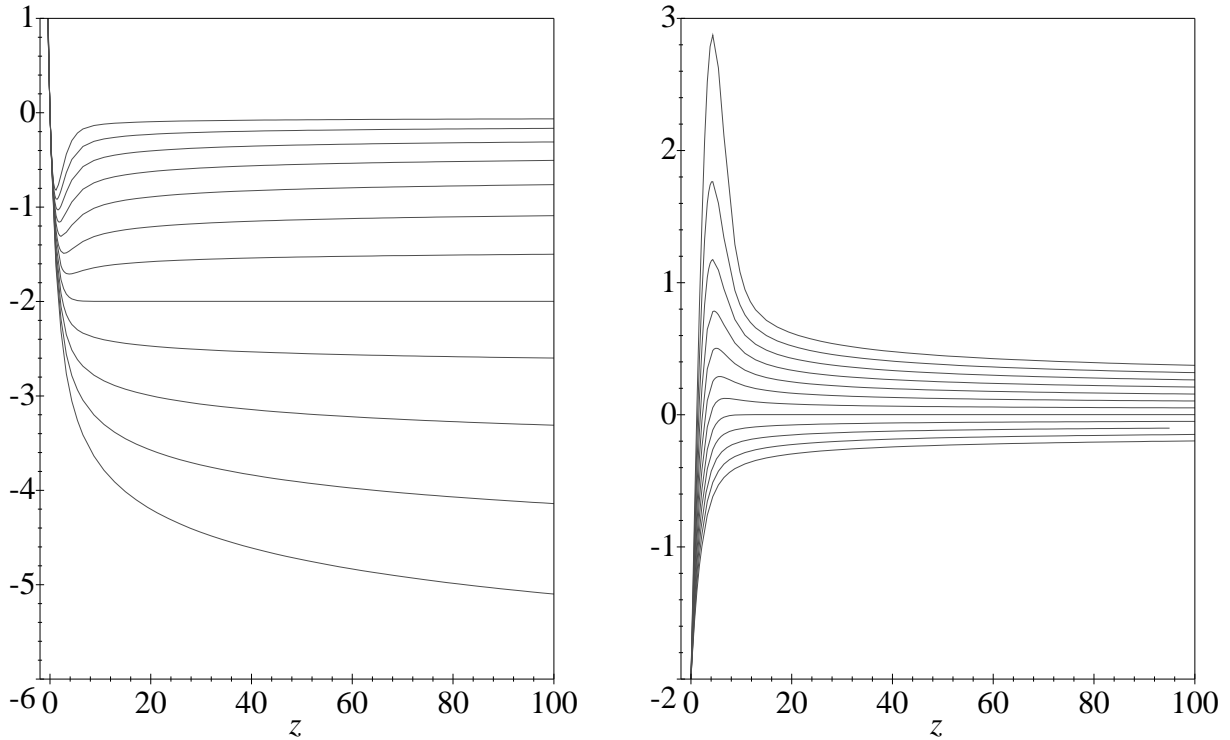


Figure 6.2: β -function (left) and ω (right) as functions of the dimensionless bare coupling z for different dimensions d : $d = 0.25, 0.5, 0.75, \dots, 3$ (from top to bottom, respectively). Note, that β always has a fixed point at $z=0$ with $\omega(0) = -\varepsilon$. Furthermore, there is a fixed point for $0 < d < 2$ at $z=\infty$ with $\omega(\infty)=0$, the latter remaining true for $d \geq 2$. In $d=2$ β tends to $-\varepsilon$ as $z \rightarrow \infty$. Above, β diverges.

where omitted terms have either one more power of $(2 - D)$ or $1/\ln z$. As shown in section 2, universal properties are given by the correction to scaling exponent ω , reading

$$\omega(z) := \frac{d\beta(g)}{dg} = \frac{d\beta(z)}{dz} \frac{1}{\frac{dg}{dz}} = -\frac{\varepsilon z}{\beta(z)} \frac{d\beta(z)}{dz}. \quad (6.43)$$

Let us first study $D = 2$. $\beta(z)$ and $\omega(z)$ are plotted on figure 6.2. We see that for $d < 2$ the β -function becomes 0 for $z \rightarrow \infty$. For $d > 2$, $\beta(z)$ has no zero, but the flow of g is still to infinity. In both cases ω is given by $\omega = \lim_{z \rightarrow \infty} \omega(z)$. Taking only the leading term in the $(2 - D)$ -expansion of $\beta(z)$, $\omega(z)$ is given by

$$\omega(z) = -\varepsilon \frac{z \frac{d}{dz} f_1^d(z)}{f_1^d(z)} = \frac{d-2}{2 \ln z} \rightarrow 0. \quad (6.44)$$

Let us now take into account the first order in $2 - D$. Then the fixed point of (6.42) is at the finite value

$$\ln z^* = \frac{2}{2 - D}. \quad (6.45)$$

Next, when trying to calculate $\omega(z)$, we face the following problem: Since we truncated the series for g at order one in $2 - D$, $\beta'(z)$ does not vanish at the fixed point, i.e. the zero of $\beta(z)$. This might lead to the conclusion that $\omega(z^*)$ is always ∞ , an absurd result. However since this is a consequence of the truncation of the series, we follow the strategy also to expand the

denominator of $\omega(z)$ in powers of $2 - D$. From (6.41) and (6.43) we obtain:

$$\omega(z) = -\varepsilon \left[\frac{z \frac{d}{dz} f_1^d(z)}{f_1^d(z)} + (2 - D) \frac{z \frac{d}{dz} \left[-\frac{d}{2} f_2^{d+2}(z) + \frac{d}{8} f_3^{d+2}(z) \right]}{f_1^d(z)} \right. \\ \left. + (2 - D) \frac{\left[\frac{d}{2} f_2^{d+2}(z) - \frac{d}{8} f_3^{d+2}(z) \right] z \frac{d}{dz} f_1^d(z)}{f_1^d(z)^2} \right]. \quad (6.46)$$

Inserting the asymptotic series, we find

$$\omega(z) = -\varepsilon \frac{d-2}{2 \ln z} + \varepsilon \frac{2-D}{2}. \quad (6.47)$$

Inserting the fixed point (6.45), we arrive at

$$\omega(z^*) = \varepsilon (2 - D) \frac{4 - d}{4}. \quad (6.48)$$

This should be checked against the exact result in $D = 1$, which reads

$$\omega(D=1) = \varepsilon. \quad (6.49)$$

Thus for $d \rightarrow 0$ our resummation-procedure gives the exact and for $d > 0$ an approximative result. Before analyzing the validity of the procedure, let us turn to the second scheme, namely the calculation in the renormalized coupling.

6.5 Calculation in the renormalized coupling

We start from $g(z)$ given in (6.38). For large z this can be approximated by

$$g(z) = \frac{(\ln z)^{d/2}}{\Gamma(\frac{d}{2}+1)} - (2 - D) \frac{d (\ln z)^{d/2+1}}{4 \Gamma(\frac{d}{2}+2)}, \quad (6.50)$$

where we only retained the leading term from each series. Also note that this formula is only valid for $d < 2$. For $d \geq 2$ additional additive constants have to be added. Using (6.50), we can write $\ln z$ as a function of g . To first order in $2 - D$, this reads

$$\ln z = \tilde{g}^{2/d} + \frac{2 - D}{2 + d} \tilde{g}^{4/d}, \quad \tilde{g} := g \Gamma(\frac{d}{2} + 1). \quad (6.51)$$

We now write the β -function in terms of \tilde{g} . Starting from (6.42) we obtain

$$\beta(\tilde{g}) = -\frac{\varepsilon}{\Gamma(\frac{d}{2})} \left[\tilde{g}^{1-2/d} - \frac{2(2-D)}{2+d} \tilde{g} \right]. \quad (6.52)$$

Fixed points are at the zeros of the β -function. The non-trivial one is at

$$\tilde{g}^* = \left[\frac{2+d}{2(2-D)} \right]^{d/2}. \quad (6.53)$$

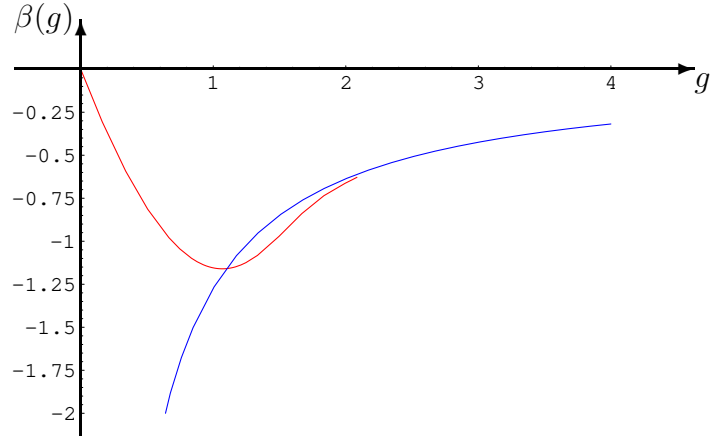


Figure 6.3: β -function in terms of the renormalized coupling g truncated at order 160, Pade-resummed, and plotting only that part for which the truncated series converges. (This can e.g. be tested by taking away the last few terms of the series.) This is compared to the asymptotic behavior (6.52) (proportional to $1/g$ for large g). d is set to 1, and we used the diagonal (80,80)-Pade approximant, which was found to converge best. (The non-resummed expression starts to diverge already at $g \approx 1.8$ at this order.)

The correction to scaling exponent ω is simply obtained by evaluating the derivative of β with respect to g at the fixed point. In terms of \tilde{g} this is

$$\begin{aligned} \omega(\tilde{g}) &= \frac{d\beta(g)}{dg} = \frac{d\beta(\tilde{g})}{d\tilde{g}} \frac{d\tilde{g}}{dg} = \Gamma\left(\frac{d}{2} + 1\right) \frac{d\beta(\tilde{g})}{d\tilde{g}} \\ &= -\varepsilon \left[\left(\frac{d}{2} - 1\right) \tilde{g}^{-2/d} - \frac{d(2-D)}{2+d} \right]. \end{aligned} \quad (6.54)$$

Inserting the fixed point \tilde{g}^* from (6.53) we find

$$\omega(\tilde{g}^*) = \varepsilon \frac{2(2-D)}{2+d}. \quad (6.55)$$

Again, this is quite close to the exact result $\omega(D=1) = \varepsilon$ in $D = 1$, and in effect exact in $D = 1$ and $d = 0$.

Let us finally point out that in the limit $D = 2$ the true asymptotic behavior of the β -function in terms of the renormalized coupling g is obtained from the completely summed series (6.27) leading to (6.52) for large g . Conversely, if one tries to invert (6.27) and truncates it taking only a finite number of orders into account, it is at least possible to reach the asymptotic regime – however, for large enough g the truncated β -function wildly oscillates and thus strongly deviates from the true behavior. In figure (6.3) the Pade-resummed truncated β -function up to order g^{160} in $d = 1$ is compared with the exact, asymptotic flow-function. One notices that the truncated β -function even though improved through a Pade-Resummation hardly gets into touch with the asymptotic regime. The same applies to the slope-function $\omega(g)$, which is not shown in fig. (6.3).

Note that the above arguments suggest quite intuitively the behavior of the exact β -function in $1 < D < 2$. Whereas for $D = 1$, the β -function is a parabola, and for $D = 2$ it decays like

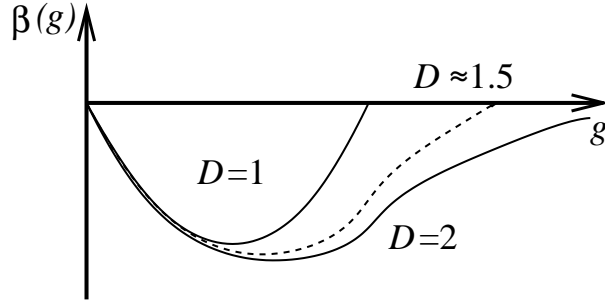


Figure 6.4: Qualitative behavior for the β -function in $D = 1$, $D = 2$ and result anticipated for $D \approx 1.5$.

a power-law for large g at least as long as $d < 2$, the β -function for values of D between these two extremes should cut the axes $\beta(g) = 0$ at a finite value of g , which for $D \rightarrow 2$ wanders off to infinity, thus by continuity forcing the exponent ω to go to 0 for $D \rightarrow 2$.

6.6 An instructive case: $d = 0$

Setting $d = 0$ in the leading order series (6.27) allows for a simple analytic expression for g as a function of z and its inversion

$$g(z) = 1 - e^{-z} \quad (6.56)$$

$$z(g) = -\ln(1 - g) . \quad (6.57)$$

This gives

$$\beta(g) = \varepsilon(1 - g) \ln(1 - g) \quad (6.58)$$

$$\omega(g) = -\varepsilon(1 + \ln(1 - g)) . \quad (6.59)$$

Fixed points are $g^* = 0$ and $g^* = 1$ with $\omega(g^*=0) = -\varepsilon$ and $\omega(g^*=1) = \infty$. Note that the latter result is an artifact of $d = 0$.

7 Discussion and conclusion

In this article, we have discussed the perturbation expansion of a D -dimensional elastic manifold interacting via a δ -interaction with a fixed point in embedding space. This calculation can be done exactly for $D = 1$, but becomes non-trivial for $D \neq 1$. Interestingly and quite surprisingly, it simplifies considerably in the limit of $D \rightarrow 2$, if one decides to work at finite ε . In that limit we were able to obtain an explicit expression for the renormalized coupling as function of the bare one, in terms of a non-trivial series. Analysis of this series shows that the fixed point lies at infinity in the bare coupling, a limit in which we were able to derive an asymptotic expansion for the renormalized coupling as a function of the bare one. This yields a vanishing exponent ω in the limit of $D \rightarrow 2$. Also it is important to note that this result is completely independent of the regularization procedure. This does no longer hold true beyond the leading order, which should be accessible to an expansion in $(2 - D)$. We here constructed its first order in a specific regularization scheme. While this reproduces qualitatively correctly

the known results in $D = 1$ (and even exactly for $d = 0$), it also shows by its dependence on the renormalization scheme (here working with the β -function either in terms of the renormalized or bare coupling) that this expansion in $(2 - D)$ is not systematic. Even though experience with this new kind of expansion is still lacking, this is likely to be caused by the use of a hard cutoff in position space while working with the correlator of an infinite membrane. It seems that only in an ε -expansion this procedure is systematic. Work is in progress [29] to study the model on a sphere or torus of finite size, such that no further infrared cutoff is necessary. This should lead to exact results beyond the leading order and provide for the crossover between polymers and membranes.

While results for the pinning problem are interesting in its own, the main motivation is certainly to obtain a better understanding of self-avoiding polymerized membranes. This model is well-behaved physically, since its fractal dimension d_f is bounded by the dimension of the embedding space $d_f < d$. Preliminary studies [29] indicate that this problem can also be attacked by the methods developed in this article. This would be very welcome to check the 2-loop calculations [27,26] and the large-order behavior [36] on one side and numerical results (e.g. [28]) on the other.

A Universal $1/r$ - repulsion law for polymers

We have shown in section 2.2 by a scaling argument that as long as $r \ll L^\nu$, the restricted partition function of a manifold pinned at one of its internal points scales as $\mathcal{Z}_\infty(r/L^\nu) \sim (r/L^\nu)^\theta$, with the contact-exponent given by (2.25). It is instructive to prove this for the special case of polymers in $d = 1$. According to (2.1) and (2.6) this corresponds to a polymer in $3d$ -space interacting with a δ -potential on a plane.

Let us start from the (bulk) polymer propagator being defined as the conditional probability of finding the internal point s' at the position r_f when starting in s at r_i . The propagator can be written as a functional integral for a restricted partition function of the free chain according to

$$\begin{aligned} \mathcal{Z}_{s,s'}(r_i|r_f) &= \int \mathcal{D}[r] \tilde{\delta}(r(s)-r_i) \tilde{\delta}(r(s')-r_f) e^{-\mathcal{H}[r]} \\ &= \int_k e^{-k^2|s'-s|+ik(r_f-r_i)} = |s'-s|^{-d/2} e^{-\frac{(r_f-r_i)^2}{4|s'-s|}}. \end{aligned} \quad (\text{A.1})$$

The propagator (A.1) possesses the Markov property

$$\mathcal{Z}_{s,s''}(r_i|r_f) = \int d^d r_m \mathcal{Z}_{s,s'}(r_i|r_m) \mathcal{Z}_{s',s''}(r_m|r_f). \quad (\text{A.2})$$

In the following we are interested in the restricted partition function (A.1) in presence of a short-range interaction modeled through a δ -potential, which is situated at the origin of the embedding space. The restricted partition function in the presence of the interaction will be denoted by $\mathcal{Z}_{s,s'}^{g_0}(r_i|r_f)$. We consider the case, where the chain is fixed at its ends, such that $s=0$ and $s'=L$. We furthermore switch to a grand-canonical ensemble and denote

$$\mathcal{Z}_\tau^{g_0}(r_i|r_f) := \int_0^\infty dL \mathcal{Z}_{0,L}^{g_0}(r_i|r_f) e^{-\tau L}, \quad (\text{A.3})$$

τ being some chemical potential. $\mathcal{Z}_\tau^{g_0}(r_i|r_f)$ can be expanded in a perturbation series in the coupling g_0 according to

$$\mathcal{Z}_\tau^{g_0}(r_i|r_f) = \sum_{n=0}^{\infty} (-g_0)^n \mathcal{Z}_\tau^{g_0,n}(r_i|r_f). \quad (\text{A.4})$$

The $\mathcal{Z}_\tau^{g_0,n}(r_i|r_f)$ are

$$\begin{aligned} \mathcal{Z}_\tau^{g_0,n}(r_i|r_f) &:= \int_0^\infty dL \int_{0 < x_1 < \dots < x_n < L} \mathcal{Z}_{0,x_1}(r_i|0) \mathcal{Z}_{x_1,x_2}(0|0) \times \dots \\ &\quad \dots \times \mathcal{Z}_{x_{n-1},x_n}(0|0) \mathcal{Z}_{x_n,L}(0|r_f) e^{-\tau L} \\ &= \left[\int_0^\infty dx e^{-x\tau} \mathcal{Z}_{0,x}(r_i, 0) \right] \left[\int_0^\infty dx e^{-x\tau} \mathcal{Z}_{0,x}(0, 0) \right]^{n-1} \left[\int_0^\infty dx e^{-x\tau} \mathcal{Z}_{0,x}(0, r_f) \right] \\ &= \mathcal{Z}_\tau^0(r_i|0) \mathcal{Z}_\tau^0(0|0)^{n-1} \mathcal{Z}_\tau^0(0|r_f), \end{aligned} \quad (\text{A.5})$$

where we have used that after integration over L , the integrals factorize; we further have defined

$$\begin{aligned} \mathcal{Z}_\tau(r_i|r_f) &= \int_0^\infty ds \mathcal{Z}_{0,s}(r_i|r_f) e^{-\tau s} \\ &= \int_0^\infty ds \int_k e^{-(k^2+\tau)s+ik(r_f-r_i)} = \int_k \frac{e^{ik(r_f-r_i)}}{k^2 + \tau}. \end{aligned} \quad (\text{A.6})$$

In $d=1$ the integration over the momenta k in (A.6) leads to

$$\mathcal{Z}_\tau(r_i|r_f)|_{d=1} = \sqrt{\frac{\pi}{\tau}} e^{-\sqrt{\tau}|r_f-r_i|}. \quad (\text{A.7})$$

Let us now look at what terms appear in the n -th order coefficient in (A.5): From the initial point of the chain a factor $\mathcal{Z}_\tau(r_i|0)$ is contributed, while the final point is coming up with $\mathcal{Z}_\tau(0|r_f)$. Furthermore, the internal points give $n-1$ powers of $\mathcal{Z}_\tau(0|0)$, where

$$\mathcal{Z}_\tau(0|0) = \sqrt{\frac{\pi}{\tau}}. \quad (\text{A.8})$$

The ($n=0$)-coefficient is special: Clearly, one has

$$\mathcal{Z}_\tau^{g_0,0}(r_i|r_f) = \mathcal{Z}_\tau(r_i|r_f). \quad (\text{A.9})$$

Inserting (A.8)-(A.9) into (A.5) we obtain for (A.4):

$$\begin{aligned} \mathcal{Z}_\tau^{g_0}(r_i|r_f) &= \sqrt{\frac{\pi}{\tau}} \left[e^{-\sqrt{\tau}|r_f-r_i|} + e^{-\sqrt{\tau}(|r_f|+|r_i|)} \sum_{n=1}^{\infty} \left(-g_0 \sqrt{\frac{\pi}{\tau}} \right)^n \right] \\ &= \sqrt{\frac{\pi}{\tau}} \left[e^{-\sqrt{\tau}|r_f-r_i|} - e^{-\sqrt{\tau}(|r_f|+|r_i|)} \frac{1}{1 + \frac{1}{g_0} \sqrt{\frac{\tau}{\pi}}} \right]. \end{aligned} \quad (\text{A.10})$$

The limit of $g_0 \rightarrow \infty$ can be taken and leaves us with the beautiful result

$$\mathcal{Z}_\tau^\infty(r_i|r_f) = \sqrt{\frac{\pi}{\tau}} \left(e^{-\sqrt{\tau}|r_f-r_i|} - e^{-\sqrt{\tau}(|r_f|+|r_i|)} \right). \quad (\text{A.11})$$

This is the propagator of a scalar field with Dirichlet boundary conditions. It has applications when studying critical phenomena of e.g. an Ising magnet in half-space [37,38]. Performing the inverse Laplace-transformation of (A.11) we arrive at

$$\mathcal{Z}_L^\infty(r_i|r_f) = \frac{1}{L^{1/2}} \left(e^{-\frac{(r_f-r_i)^2}{4|L|}} - e^{-\frac{(|r_f|+|r_i|)^2}{4|L|}} \right). \quad (\text{A.12})$$

We conclude that a δ - potential acting in a hyper-plane suppresses all configurations which penetrate or touch it, when taking its amplitude to infinity.

Finally, in order to prove the universal repulsion law, we start from (A.12) and integrate over all final positions r_f :

$$\mathcal{Z}_L^\infty(r_i) = \int_{-\infty}^{\infty} dr_f \mathcal{Z}_L^\infty(r_i|r_f) = 2\sqrt{\pi} \left(1 - \operatorname{erf} \frac{|r_i|}{2\sqrt{L}} \right), \quad (\text{A.13})$$

erf denoting the error function. For small arguments we have

$$1 - \operatorname{erf}(x) \sim x. \quad (\text{A.14})$$

Furthermore, $\mathcal{Z}_L^\infty(r_i)$ denotes the restricted partition function of a chain pinned at one of its ends in r_i . To obtain $\mathcal{Z}_\infty(r/L^\nu)$ in (2.23) we have to evaluate:

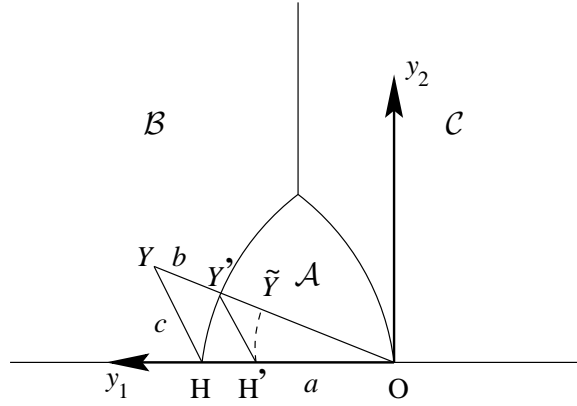
$$\mathcal{Z}_\infty(r/L^\nu) = \frac{1}{L} \int_0^L ds \mathcal{Z}_s^\infty(r) \mathcal{Z}_{L-s}^\infty(r) \sim \left(\frac{r}{\sqrt{L}} \right)^2 \quad (\text{A.15})$$

according to (A.14) in the scaling regime $r \ll L^{1/2}$. We thus find that $\theta = 2$, which confirms (2.25) for $D = 1$ and $d = 1$. The above proof can be extended to arbitrary dimensions $0 < d < 2$, where $\varepsilon > 0$ for polymers. Then, $\theta = 4 - 2d$.

It would be nice to make the same arguments for membranes. However, the proof is based on a drastic simplification, which only occurs in $D=1$ and shows up in the factorizability of loop diagrams as in (A.5). This has no extension to manifolds of internal dimension $D > 1$.

B Conformal mapping of the sectors

In order to calculate the two-loop diagram efficiently, one wants to write it as an integral over a finite domain only. To do so we need the technique of conformal mapping of the sectors, which also serves for analytically continuing the measure of integration to internal dimensions $D < 1$. This technique has been extensively used and well documented in the context of self-avoiding tethered membranes [30,27,4], but we repeat the presentation here for completeness.


 Figure B.1: The sectors \mathcal{A} , \mathcal{B} and \mathcal{C}

Generally, in evaluating the three-point divergences we need to integrate over some domain in the upper half-plane (see 4.11). The measure of integration reads

$$\int_y = \frac{S_{D-1}}{S_D} \int_{-\infty}^{\infty} dy_1 \int_0^{\infty} dy_2 (y_2)^{D-2} \quad (\text{B.1})$$

and the integrand is a function f of the three distances a , b and c between the points $O = (0, 0)$, $H = (-L, 0)$ and $Y = (y_1, y_2)$, given explicitly by (see fig. B.1)

$$a = L = \text{fixed}, \quad b = \sqrt{(y_1)^2 + (y_2)^2}, \quad c = \sqrt{(L-y_1)^2 + (y_2)^2}. \quad (\text{B.2})$$

In our problem f is homogeneous, of degree λ , but not necessarily symmetric:

$$f(\kappa a, \kappa b, \kappa c) = \kappa^{-\lambda} f(a, b, c). \quad (\text{B.3})$$

Let us now explicitly show, how sectors can be mapped onto each other. Specializing to the mapping $\mathcal{B} \rightarrow \mathcal{A}$ we choose a coordinate system as given in figure (B.1). The mapping $\mathcal{B} \rightarrow \mathcal{A}$ is mediated by a special conformal transformation, the inversion with respect to the circle around O and radius L . In complex coordinates this is (\bar{Y} is the complex conjugate of Y)

$$Y \longrightarrow \tilde{Y} = \frac{L^2}{\bar{Y}} = Y \frac{L^2}{b^2} \Leftrightarrow Y = \tilde{Y} \frac{L^2}{b^2} \quad (\text{B.4})$$

such that

$$\begin{pmatrix} y_1 \\ y_2 \end{pmatrix} \longrightarrow \begin{pmatrix} \tilde{y}_1 \\ \tilde{y}_2 \end{pmatrix} = \begin{pmatrix} \frac{y_1 L^2}{b^2} \\ \frac{y_2 L^2}{b^2} \end{pmatrix} \Leftrightarrow \begin{pmatrix} y_1 \\ y_2 \end{pmatrix} = \begin{pmatrix} \frac{\tilde{y}_1 L^2}{b^2} \\ \frac{\tilde{y}_2 L^2}{b^2} \end{pmatrix}. \quad (\text{B.5})$$

This change of coordinates gives a Jacobian for the measure (B.1)

$$\left(\frac{L^2}{b^2} \right)^D. \quad (\text{B.6})$$

It can easily be seen that the mapping $\mathcal{B} \rightarrow \mathcal{A}$ is one to one: First, be $Y=(y_1, y_2) \in \mathcal{B}$, that is $b > L$ and $b > c$. Then,

$$\tilde{c}^2 = ((\tilde{y}_1 - L)^2 + (\tilde{y}_2)^2) = \frac{L^4 - 2y_1L^3 + b^2L^2}{b^2} = L^2 \frac{c^2}{b^2} < L^2 \quad (\text{B.7})$$

and

$$\tilde{b}^2 = L^2 \frac{L^2}{b^2} < L^2. \quad (\text{B.8})$$

Since $\tilde{b}^2, \tilde{c}^2 < L^2$, $\tilde{Y} \in \mathcal{A}$. Second, for the inverse mapping, $Y(\tilde{Y} \in \mathcal{A}) \in \mathcal{B}$ is checked as follows:

$$c^2 = b^2 + L^2 - 2y_1L = b^2 + L^2 - 2\tilde{y}_1 \frac{L^3}{\tilde{b}^2} < b^2, \quad (\text{B.9})$$

since

$$c^2 = \tilde{b}^2 - 2\tilde{y}_1L + L^2 < L^2 \Leftrightarrow L^2 - 2\tilde{y}_1 \frac{L^3}{\tilde{b}^2} < 0$$

and

$$b^2 = L^2 \frac{L^2}{\tilde{b}^2} > L^2. \quad (\text{B.10})$$

Since $b > L$ and $b > c$, $Y \in \mathcal{B}$. Finally, let us look at how the whole integral transforms. First inserting the transformed variables including the Jacobian (B.6) and second using the homogeneity (B.3), we arrive at

$$\int_{Y \in \mathcal{B}} f(a = L, b, c) = \int_{\tilde{Y} \in \mathcal{A}} \left(\frac{L}{\tilde{b}}\right)^{2D} f\left(L, \frac{L^2}{\tilde{b}}, \frac{\tilde{c}L}{\tilde{b}}\right) = \int_{\tilde{Y} \in \mathcal{A}} \left(\frac{L}{\tilde{b}}\right)^{2D-\lambda} f(\tilde{b}, \tilde{a} = L, \tilde{c}). \quad (\text{B.11})$$

Let us restate the above calculation in a completely geometric interpretation as sketched in the figure. The mapping consists of two steps:

- The rescaling with respect to O by a factor L/b which maps Y onto Y' and H onto H' . (B.3) implies that f is changed by a factor $\left(\frac{L}{b}\right)^{-\lambda}$.
- A mirror operation, which maps Y' onto H and H' onto \tilde{Y} , leaving invariant the origin O . This operation is a permutation of the first two arguments of f .

The mapping $Y \rightarrow \tilde{Y}$ corresponds to the special conformal transformation (B.4). Analogously, we find that

$$\int_{Y \in \mathcal{C}} f(a = L, b, c) = \int_{\tilde{Y} \in \mathcal{A}} \left(\frac{L}{\tilde{c}}\right)^{2D-\lambda} f(\tilde{c}, \tilde{b}, \tilde{a} = L). \quad (\text{B.12})$$

Acknowledgements

It is a pleasure to thank R. Blossey, F. David, H.W. Diehl, M. Kardar, and L. Schäfer for useful discussions. The clarity of this presentation has profited from a critical reading by H.W. Diehl. We are grateful to Andreas Ludwig for persisting questions, and his never tiring efforts to understand the limit of $D \rightarrow 2$. This work has been supported by the DFG through the Leibniz program Di 378/2-1, under Heisenberg grant Wi 1932/1-1, and NSF grant PHY99-07949.

R References

- [1] L. Schäfer, *Excluded Volume Effects in Polymer Solutions*, Springer Verlag, Berlin, Heidelberg, 1999.
- [2] G. Blatter, M.V. Feigel'man, V.B. Geshkenbein, A.I. Larkin and V.M. Vinokur, *Vortices in high-temperature superconductors*, Rev. Mod. Phys. **66** (1994) 1125.
- [3] M. Kardar, G. Parisi and Y.-C. Zhang, *Dynamic scaling of growing interfaces*, Phys. Rev. Lett. **56** (1986) 889–892.
- [4] K.J. Wiese, *Polymerized membranes, a review*. Volume 19 of *Phase Transitions and Critical Phenomena*, Academic Press, London, 1999.
- [5] D.B. Abraham, *Solvable model with a roughening transition for a planar ising ferromagnet*, Phys. Rev. Lett. **44** (1980) 1165–1168.
- [6] P.J. Upton, *Exact interface model for wetting in the planar ising model*, Phys. Rev. E **60** (1999) 3475–3478.
- [7] H. Nakanishi and M.E. Fisher, *Multicriticality of wetting, prewetting, and surface transition*, Phys. Rev. Lett. **49** (1982) 1565–1568.
- [8] B.I. Halperin E. Brézin and S. Leibler, *Critical wetting in three dimensions*, Phys. Rev. Lett. **50** (1983) 1387.
- [9] R. Lipowsky, D.M. Kroll and R.K.P. Zia, *Effective field theory for interface delocalization transitions*, Phys. Rev. B **27** (1983) 4499–4502.
- [10] D.M. Kroll, R. Lipowsky and R.K.P. Zia, *Universality classes for critical wetting*, Phys. Rev. B **32** (1985) 1862.
- [11] D.S. Fisher and D.A. Huse, *Wetting transitions: a functional renormalization-group approach*, Phys. Rev. B **32** (1985) 247–56.
- [12] R. Lipowsky and M.E. Fisher, *Scaling regimes and functional renormalization for wetting transitions*, Phys. Rev. B **36** (1987) 2126–2241.
- [13] F. David and S. Leibler, *Multicritical unbinding phenomena and nonlinear functional renormalization group*, Phys. Rev. B **41** (1990) 12926–9.
- [14] G. Forgas, R. Lipowsky and T.M. Nieuwenhuizen, *The behaviour of interfaces in ordered and disordered systems*. Volume 14 of *Phase Transitions and Critical Phenomena*, pages 136–376, Academic Press London, 1991.
- [15] B. Duplantier, *Interaction of crumpled manifolds with euclidean elements*, Phys. Rev. Lett. **62** (1989) 2337.
- [16] F. David, B. Duplantier and E. Guitter, *Renormalization of crumpled manifolds*, Phys. Rev. Lett. **70** (1993) 2205.

- [17] F. David, B. Duplantier and E. Guitter, *Renormalization theory for interacting crumpled manifolds*, Nucl. Phys. **B 394** (1993) 555–664.
- [18] Y. Kantor and D.R. Nelson, *Crumpling transition in polymerized membranes*, Phys. Rev. Lett. **58** (1987) 2774–2777.
- [19] Y. Kantor and D.R. Nelson, *Phase transitions in flexible polymeric surfaces*, Phys. Rev. **A 36** (1987) 4020–4032.
- [20] Y. Kantor, M. Kardar and D.R. Nelson, *Statistical mechanics of tethered surfaces*, Phys. Rev. Lett. **57** (1986) 791–795.
- [21] Y. Kantor, M. Kardar and D.R. Nelson, *Tethered surfaces: Statics and dynamics*, Phys. Rev. **A 35** (1987) 3056–3071.
- [22] M. Kardar and D.R. Nelson, *ε expansions for crumpled manifolds*, Phys. Rev. Lett. **58** (1987) 1289 and 2280 E.
- [23] J.A. Aronovitz and T.C. Lubensky, *Fluctuations of solid membranes*, Phys. Rev. Lett. **60** (1988) 2634–2637.
- [24] F. David, B. Duplantier and E. Guitter, *Renormalization and hyperscaling for self-avoiding manifold models*, Phys. Rev. Lett. **72** (1994) 311.
- [25] F. David, B. Duplantier and E. Guitter, *Renormalization theory for the self-avoiding polymerized membranes*, cond-mat/**9702136** (1997).
- [26] F. David and K.J. Wiese, *Scaling of self-avoiding tethered membranes: 2-loop renormalization group results*, Phys. Rev. Lett. **76** (1996) 4564.
- [27] K.J. Wiese and F. David, *New renormalization group results for scaling of self-avoiding tethered membranes*, Nucl. Phys. **B 487** (1997) 529–632.
- [28] G. Thorleifsson M. Bowick, A. Cacciuto and A. Travesset, *Universality classes of self-avoiding fixed-connectivity membranes*, Eur. Phys. J. **E 5** (2001) 149.
- [29] H. Pinnow and K.J. Wiese, work in progress.
- [30] K.J. Wiese and F. David, *Self-avoiding tethered membranes at the tricritical point*, Nucl. Phys. **B 450** (1995) 495–557.
- [31] T. Hwa, *Generalized ε expansion for self-avoiding tethered manifolds*, Phys. Rev. **A 41** (1990) 1751–1756.
- [32] M. Lässig and R. Lipowsky, *Critical roughening of interfaces: a new class of renormalizable field theories*, Phys. Rev. Lett. **70** (1993) 1131–4.
- [33] M. Goulian, *The gaussian approximation for self-avoiding tethered surfaces*, J. Phys. II France **1** (1991) 1327–1330.

- [34] P. Le Doussal, *Tethered membranes with long-range self-avoidance: large dimension limit*, J. Phys. A **25** (1992) 469–476.
- [35] E. Gitter and J. Palmeri, *Tethered membranes with long-range interaction*, Phys. Rev. A **45** (1992) 734–744.
- [36] F. David and K.J. Wiese, *Large orders for self-avoiding membranes*, Nucl. Phys. B **535** (1998) 555–595.
- [37] H.W. Diehl, *Field-theoretical approach to critical behaviour of surfaces*. Volume 10 of *Phase Transitions and Critical Phenomena*, pages 76–267, Academic Press London, 1986.
- [38] E. Eisenriegler, K. Kremer and K. Binder, *Adsorption of polymer chains at surfaces: scaling and Monte-Carlo analysis*, J. of Chem. Phys. **77** (1982) 6296.